Discontinuous Aligned Carbon Fiber Intermediates for Automotive and Related Applications

Authors: Robert Conforti, Ganesh Deka, Neenah Paper

Uday Vaidya, John Unser, IACMI

Date: September 15, 2022
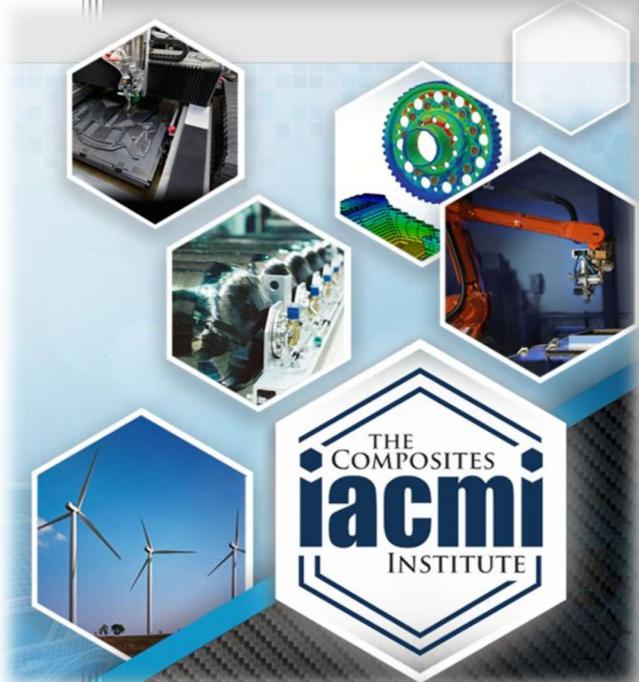
Final Technical Report

PA16-0349-6.11-01

**Approved for Public Release.
Distribution is Unlimited.**

THE INSTITUTE FOR
IACMI
Advanced Composites
Manufacturing Innovation
THE COMPOSITES INSTITUTE

U.S. DEPARTMENT OF
ENERGY

Discontinuous Aligned Carbon Fiber Intermediates for Automotive and Related Applications

Principal Investigator: Robert Conforti, Ganesh Deka

Organization: Neenah Paper

Address: 70 Front Street, West Springfield, MA 01089
Phone: (802)779-5467
Email: robert.conforti@neenah.com

Co-authors:
- Uday Vaidya, PhD (Chief Technology Officer, IACMI; UT-ORNL Governor's Chair in Advanced Composites Manufacturing
- Soydan Ozcan, Oak Ridge National Laboratory
- John Unser, Technology Impact Manager, IACMI-The Composites Institute

Approved For Public Release

TABLE OF CONTENTS

LISTS

List of Acronyms

PP – polypropylene
PA6 – polyamide-6 (nylon)
CF – carbon fiber
CD – cross-direction
MD – machine direction
wt% - Weight percent
P4 – programmable preform placement process
WL – wet-laid
UT- University of Tennessee
IACMI – Institute for Advanced Composites Manufacturing Innovation
ORNL – Oak Ridge National Laboratory

List of Figures

List of Tables

List of Appendices

N/A

1. EXECUTIVE SUMMARY

This work focused on preferentially aligning discontinuous carbon fibers in wet-laid or air-laid processes. It is well known that aligned fibers provides higher directional strength and stiffness. Discontinuous fibers further allow higher degree of draw and formability as the gaps in the fibers allow for higher material movement. The current processes are limited in their ability to align carbon fibers during processing. The aligned fibers have several benefits - (a) in applications where chopped fibers can replace continuous fibers for targeted strength and stiffness metrics, but at a substantially reduced cost; (b) they can tolerate deeper draws than continuous fiber composites in thermo-stamping and compression molding processes; (c) they can be tailored for pultrusion and unidirectional applications. Although pultrusion is primarily a process that adopts continuous fibers, stitch bonded entangled discontinuous fibers can provide unique intermediates. This is analogous to natural coir fibers which get aligned and entangled to produce ropes/rods for example, (d) they can be processed in cross-ply and multi-directional formats, like composite laminates. In this work Neenah Paper partnered with IACMI, UT and ORNL to evaluate structure-process-property relationships with Zoltek carbon fiber. A few process parameters such as machine speed, weight basis, fiber length, effect of fiber sizing, direction of mat lay-up etc. were investigated. The produced mats were converted to thermoplastic composite laminates using polyamide 6 (PA6, nylon) resin. The specific objective of this project is to produce a wet-laid nonwoven carbon fiber mat with a high degree of unidirectional fiber alignment, using discontinuous carbon fibers. The report provides details about the processing, characterization, and lower-upper bound properties.

2. INTRODUCTION

An intermediate form in which the fibers are discontinuous, yet aligned like continuous fiber prepreg is desirable and can provide several benefits, such as (a) in applications where chopped fibers can replace continuous fibers for targeted strength and stiffness metrics, but at a substantially reduced cost; (b) they can tolerate deeper draws than continuous fiber composites in thermo-stamping and compression molding processes; (c) they are ideal for pultrusion and unidirectional applications; (d) they can be processed in cross-ply and multi-directional formats, similar to laminates.

The ability to control the fiber orientation allows for the specific tailoring of the mechanical properties of the resulting mat. Specifically, control of fiber orientation allows the mat to be tailored to the application and to the specific process. The process(es) can be tailored to low-cost textile- based carbon fibers as well as reclaimed carbon fibers from various recycling processes. Additionally, an optimized discontinuous aligned fiber mat may allow for broader application of composite materials in the automotive and other price-sensitive markets.   The lower cost fiber and the higher production speeds of the intermediate mats would result in lower cost intermediates.

This work leveraged Neenah's patented dispersion technology, in combination with its proprietary process for producing wet-laid carbon fiber non-wovens. The process conditions and equipment

were modified and optimized to maximize fiber dispersion and machine direction fiber alignment to produce a carbon fiber mat(s) with 0.5" and 1.0" aligned fibers These mats are compatible with thermoset and thermosetting resins. To this point, no prior process development work, or combination thereof had focused on aligned fibers from wet laid processes relevant to automotive use. A limited amount of prior work focused on aerospace applications with higher cost and throughput tolerance metrics than allowable in automotive high-volume markets[1].

As the wet mat is drained through the porous forming surface, it may also form a gradient structure because of draining from one direction and compacting as the mat is formed. Thus, the choice of suspension type is a critical aspect of the process and the research team identified proper suspension for the process. In addition, a sizing may also be applied by curtain or other means to improve wet-out of fibrous mat, and therefore reduce void volume in the final product.

Preliminary lab data showed that the plurality of carbon fibers is substantially aligned after the wet laid process, due to the typical fiber alignment of synthetic fibers in a wet laid web which has more fibers oriented in one direction than in any other directions. To control fiber placement and entanglement, the dispersion of the cluster of fiber tows can be manipulated by adding a dispersing aid such as a flocculant and further enhancement can be obtained by also adding a specific surfactant.

To adopt the wet-laid process for forming carbon fibers mats, further modification of current pilot scale equipment originally designed for cellulosic fibers is required. Improvements are needed in bonding agent delivery system, pressing rollers, and drying system to handle the synthetic carbon fibers properly. Researchers will optimize equipment features in conjunction with process parameters.

3   BACKGROUND

Neenah paper, Inc. has been granted two patents on the dispersion of carbon fiber tows in wet-laid manufacturing processes. The wet laid nonwoven carbon fiber mats have been molded into composites with thermoset and thermoplastic resins. These patents describe techniques used to make uniform dispersions of fibers from filament tows to improve strength of the resulting mats. No previous work has been done by Neenah in aligning these fibers in one direction. This project involves building upon Neenah's patented dispersion technology, incorporating fibers of 0.5" to 1.0" in length, in combination with defined manufacturing process improvements targeted at imparting a high degree of unidirectional fiber alignment into the resulting mat (in the direction of the web movement /machine direction). The method is an improvement of the wet-laid process in paper making, modifying it for wet-laid carbon fiber mats. The current process will be modified

---

[1] https://www.mogulsb.com/en/applications/aerospace

to form an open carbon fiber network within the mat during the wet laid process of the aqueous suspension/slurry.

There are several methods currently being practiced in producing aligned, discontinuous fibers. The aerospace industry has adopted stretch broken carbon fibers that are analogous to discontinuous aligned fibers, but the custom process they use to produce this discontinuity in the continuous fibers is cost-prohibitive for automotive applications. Other methods include the use of electrical fields, ultrasonic assembly, P4 and additive printing. These methods, while somewhat reasonable, are not practical or economically viable methods to produce the mats in forms acceptable to the automotive and consumer industries.

The specific objective of this project was to investigate wet-laid nonwoven carbon fiber mat with a high degree of unidirectional fiber alignment, using discontinuous carbon fibers.

3.1 Recap of Proposed Tasks and Milestones

This work was conducted against these proposed tasks and milestones, and they are listed below.

Subtask 6.11.1 Project Management

Milestone 6.11.2.1 Presentation of a brief describing experimentation and selection dispersant as well as process conditions that provide optimum dispersion resulting in a uniform distribution of fibers in a wet laid nonwoven mat in a chosen basis weight within the range 50-100gsm.

Subtask 6.11.2: Fiber alignment studies

Milestone 6.11.2.2 Using the technique as defined in subtask 6.11.5 and using 12mm long carbon fiber, demonstrate that ≥ 25% of carbon fibers is aligned in machine direction in a single chosen aerial basis weight within the range of 50-100gsm. Produce a mat targeting 500 gsm and characterize how alignment changes through thickness of the mat using technique as defined in Subtask 6.11.5.

Milestone 6.11.2.3 Using the technique as defined in subtask 6.11.5 and using 12mm long carbon fiber, demonstrate that ≥ 50% of carbon fibers is aligned in machine direction in a single chosen aerial basis weight within the range of 50-100gsm. Using the technique as defined in Subtask 6.11.5 and using 18 and 25mm fibers, determine if percent of carbon fiber alignment changes with length of fibers.

Subtask 6.11.3: Surface modification

Milestone 6.11.3.1 The results of the surface modification and compounding experiments and the analyses to determine suitability of aligned fiber mats for use will be reported to DOE.

Milestone 6.11.3.2 Can form a satisfactory surface treatment on carbon fiber mats that contain > 7% atomic oxygen to carbon ratio on the carbon fiber surface from samples taken from the center and surface of these mats. Surface properties will be characterized using XPS and will be shown with 6 samples from each center and surface locations of mats.

Subtask 6.11.4 Produce Molding Products using Vacuum Infusion

Milestone 6.11.4.1 Three 12" x 12" panels up to 3mm thickness will be molded using aligned, nonaligned, and continuous fiber mats.

Milestone 6.11.4.2 Brief results of business case analysis to project team and DOE

Go/No-Go 6.11.2 Production of 12" x 12" mats with aerial density of up to 150 gsm with 40% alignment in one direction.

Subtask 6.11.5 Characterization Support for Technical Tasks

Milestone 6.11.5.1 Fiber angle measuring technique will be developed.

Milestone 6.11.5.2 Report generated that is comprised of product characterization results from tests performed in previous subtasks.

4 MATERIALS AND METHODS

The goal of this project was to demonstrate repeatedly reliable production of mats with uniform distribution and with some degree of fiber alignment, and the parameters to control such alignment. This will define the extent of product performance enhancement that has been achieved from such unidirectional fiber alignment. The parameters that control fiber alignment such as machine speed (FPM), basis weight of the mats, carbon fiber length (12mm and 25mm), and repeatability of the mat production are evaluated in this study.

Carbon fiber mats from Neenah were cut 12" X 12" and stacked and epoxy resin was infused under vacuum to form panels. Epoxy resin used in this project was provided by Huntsman corporation, (product name Aradur and Araldite). The infusion uses atmospheric pressure to drive resin into a stack of dry materials that are laid into a mold to which vacuum is applied before resin is introduced under vacuum. The panel thickness was ~3mm after the complete cure of the resin.

Initial mechanical characterization and microscopy imaging revealed that the consolidated panels did not enable the expected fiber volume fraction (40 volume %). Therefore, the process was modified to enhance the fiber volume fraction and thereby validate mechanical properties. The modification involved addition of a compression molding step following resin infusion. Once a complete vacuum is achieved and resin is sucked by mats, the entire setup is transferred to a compression molding press. Fibers and resin under vacuum are pressed under 413 Psi pressure at 50°C for 24 hours. The number of mats stacked were adjusted to achieve the panel thickness of 3mm. This process enabled approximately 40% volume fractions of fibers in the consolidated

panel. Therefore, this process was used to investigate the effect of various parameters affecting the

Sized fiber mats used for resin infusion

Vacuum assisted resin transfer molding (VARTM)

Compression molding

Three-point bend testing

Test specimens cut from fabricated plates

Consolidated plate. Samples cut in machine direction (MD) and cross-direction (CD)
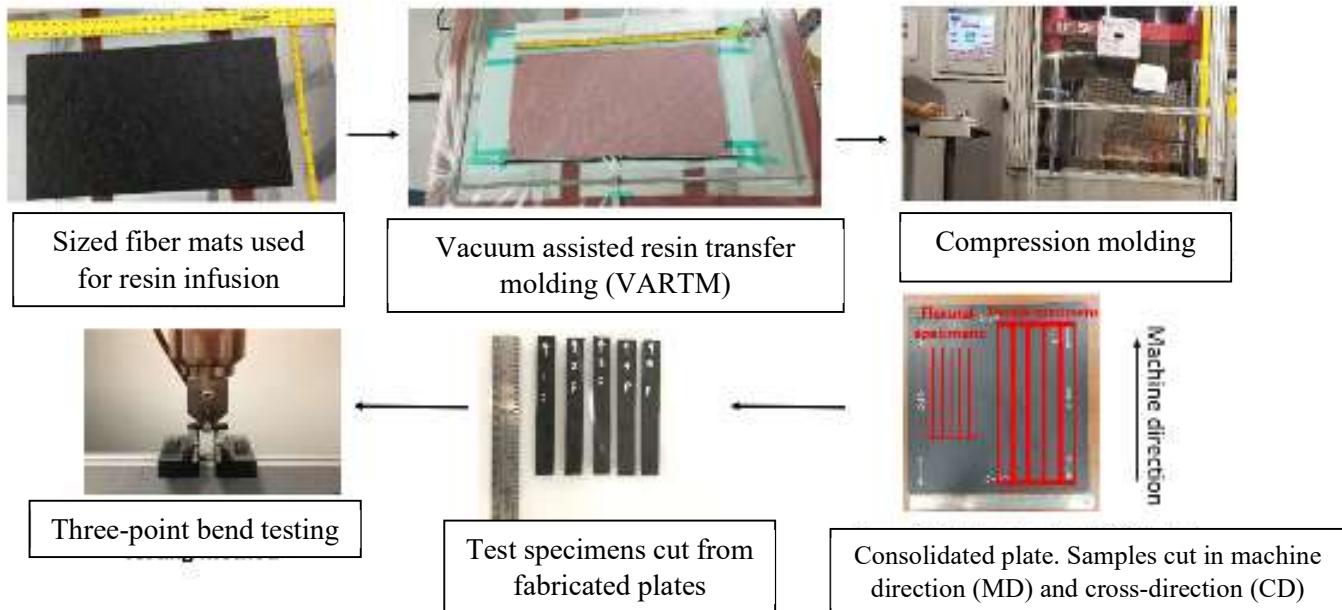
fiber alignment. Mechanical characterization includes flexural strength and tensile strength data generation. The schematic of the fabrication process and characterization is shown in figure 1.

Figure 1. Schematic of fabrication and characterization of carbon fiber composites

Neenah mats from eight different experiments were provided for mechanical property evaluation. To set baseline for the mechanical properties, carbon fiber mats with random fiber orientation via wet laid process and panels were consolidated at the University of Tennessee (UT). Mats with both sized and unsized carbon fibers were fabricated. The sized carbon fiber mats revealed uneven fiber distribution. This is thought to occur due to the higher surface tension from the sized fibers hence higher resistant to alignment. The sizing helps fiber-matrix wet out but increases the stiffness of the fiber, hence less flexibility to align. Therefore, mats with unsized carbon fibers were used for panel fabrication. Figure 2 shows the schematic of the wet laid fabrication process. The key materials and process parameters in the wet laid process were the fiber length, mixing speeds, amount of time in water, and time to drain.

Feeding raw materials

Chaotic advection for dispersion

CF mats after dispersion

CF mat after drying

Mat drying
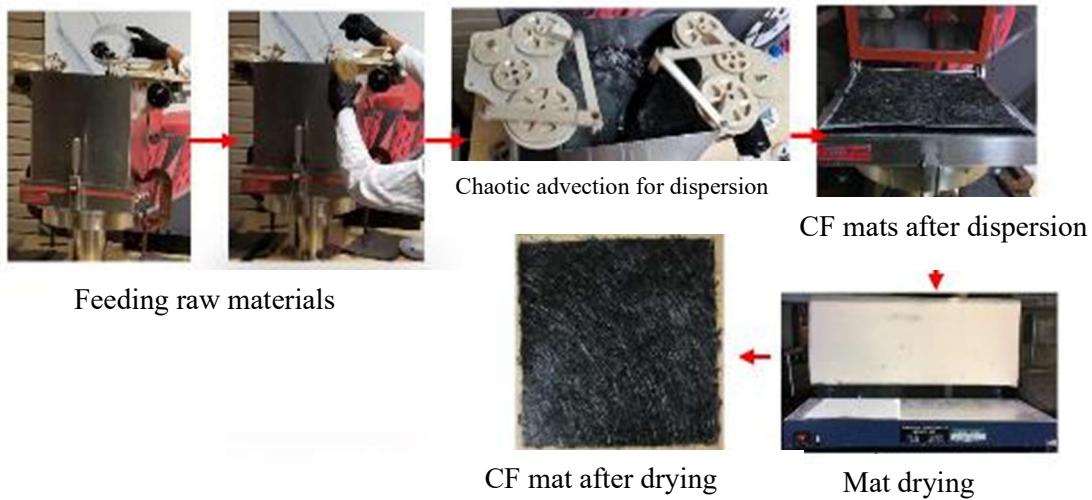
Figure 2. Fabrication of randomly oriented fiber mats via wet-laid process

5 RESULTS AND DISCUSSION

The panels fabricated were characterized with Thermogravimetric analysis (TGA) to determine the fiber volume % in the panel. These properties were normalized to 40 vol. % to have uniformity in fiber volume % while comparing mechanical properties. Also, properties were characterized in two directions, machine direction (MD) and cross direction (CD). MD corresponds to the warp direction and CD is the weft direction akin to continuous fiber terminology. Note that the effort of Neenah was to align fibers in MD.

5.1 Effect of machine speed

The effect of machine speed during mat production is the first parameter considered for mechanical property evaluation. Mechanical properties of panels from mats produced from various machine speeds i.e., 50 ft/min (Expt#2), 100 ft/min (Expt#3), 200 (Expt#4) and 300 ft/min (Expt# 5) were compared with baseline mats produced by UT (control), Neenah (Expt#1) and continuous carbon fiber composites. The detailed flexural and tensile properties are shown in Figure 3 and 4. From the data, the panels from mats produced at 300 ft/min (Expt#5) showed better flexural and tensile properties in comparison to mats produced at lower machine speeds.

5.2 Effect of basis weight

Basis weight refers to the grams per square meter commonly known as gsm in the industry. The gsm is used as a metric to quantify the areal density of the mat and provides an indication of how well the mat may respond in a process like compression molding, vacuum forming etc. For e.g., a 50 gsm is very light and conformable, a 500 gsm is more dense and less conformable. The effect of basis weight of the mats was used as another parameter considered for mechanical property evaluation. Mechanical properties of panels from mats produced from various gsm i.e., 68 gsm (Expt#12), 88 gsm (Expt#2) and 178 gsm (Expt#7-1) were compared with each other. The detailed flexural and tensile properties are shown in Figure 5 and 6. From the data, the panels from mats from 68 gsm (Expt#12) and 88 gsm (Expt#2) showed better flexural and tensile properties in comparison to mats produced at higher basis weight 178 gsm (Expt#7-1). It can be surmised that higher basis weight translates into lower mechanical properties. This can be attributed to randomized distribution through the thickness for higher basis weight mat. For lower basis weight the in-plane distribution favors narrow fiber distribution (less three-dimensional effects of fiber movement), which is thought to result in this response.

5.3 Effect of fiber length

The effect of fiber length of carbon fiber used for mat production was considered for mechanical properties evaluation. Mechanical properties of panels from mats produced using two fiber lengths 12mm and 25mm are compared with each other. The detailed flexural and tensile properties are shown in figure 7 and 8. Figure 7 illustrates comparison for # 31 and #32 respectively. Figure 8 illustrates comparison for # 4 and #11 respectively. No significant difference in tensile and flexural strength was observed as an effect of fiber length. However, the panels from mats produced using 12 mm fiber length (Expt#4) showed better flexural and tensile modulus in comparison to mats produced from 25 mm fiber length (Expt#11). Fiber entanglement due to increased fiber length in the mats could result in lower modulus.

5.4 Repeatability

The mats were produced by Neenah in two batches, one in February 2019 and the other in August 2018. The initial trials in August 2018 were to produce the mats reliably with uniform fiber distribution and with some degree of fiber alignment. In trials from February 2019, the learnings from the August 2018 trials were used to optimize the parameters and produce mats with same or higher degree of alignment. Mechanical property evaluation was conducted to investigate the repeatability of Neenah's consistency in producing mats. The detailed flexural and tensile properties are shown in figure 9 and 10. In Figures 9 and 10 the identifier -R2 indicates these results are from the second set of trials conducted in Feb 2019 (in comparison to August 2018). There was overall improvement (up to 25%) in strength and modulus for the MD comparing Aug 2018 to Feb 2019 trials. In contrast the CD values exhibited slight reduction from Aug 2018 to Feb 2019 trials. This needs further investigation. However, it appears that additional entanglement of fibers in the MD configurations provide the observed enhancement. This study did not attempt to further investigate the material microstructure, which is a subject of a following peer-reviewed journal paper being compiled by the authors.

5.5 Sizing study

Wet laid mats produced by Neenah have no surface sizing, this allows for a choice of separate surface treatment (sizing), depending on the final product design to be used during composite manufacturing. In this study, the fibers were surface treated with epoxy sizing to promote adhesion to epoxy resin. The objective of this task is to select the fiber sizing chemical formulation and processes for optimum fiber wetting and subsequent composite performance properties. The two epoxy sizing agents investigated in this study are sizing agent 1: 181291IX and sizing agent 2: EP871EU from Michelman Inc. The sizing chemistry and formulations were not shared by Michelman Inc. due to proprietary reasons. Sizing of mats included dipping of the mats in the sizing solution and drying them at 80°C for 24 hours. TGA studies reveal that the sizing concentration achieved was 1- 1.5%. Detailed tensile and flexural properties are presented in figure 11 and 12. Per data, no significant effect was observed in mechanical properties of the panels with and without sizing. This could be due to incompatibility of the sizing chemistries with the carbon fiber mats. Further investigation in choosing appropriate sizing chemistries is required.

5.6 Summary of Mechanical Characterization

The following observations can be made from the mechanical characterization data. 1) Higher mechanical properties were observed for the mats made at higher machine speed i.e.., 300 ft/min 2) Higher mechanical properties were observed for mats with 68 gsm and 88 gsm in comparison to mats with 178 gsm. It can be summarized that higher basis weight translates into lower mechanical properties. 3) Fiber length has no effect on flexural and tensile strength, however, the panels from mats produced using 12 mm fiber length showed better flexural and tensile modulus in comparison to mats produced from 25 mm fiber length 4) Repeatability study revealed similar trend in mechanical properties for the studied systems from February 2019 and August 2018 trials. 5) The sizing formulations do influence the mechanical properties in comparison to unsized data as seen from Fig 11. Therefore, mats produced from Expt#5 from August 2018 trial with basis weight of 84 gsm, fiber length 12mm and machine speed 300 FPM showed better flexural properties in comparison to panels made from all other experiments and control specimen.

(a)

(b)
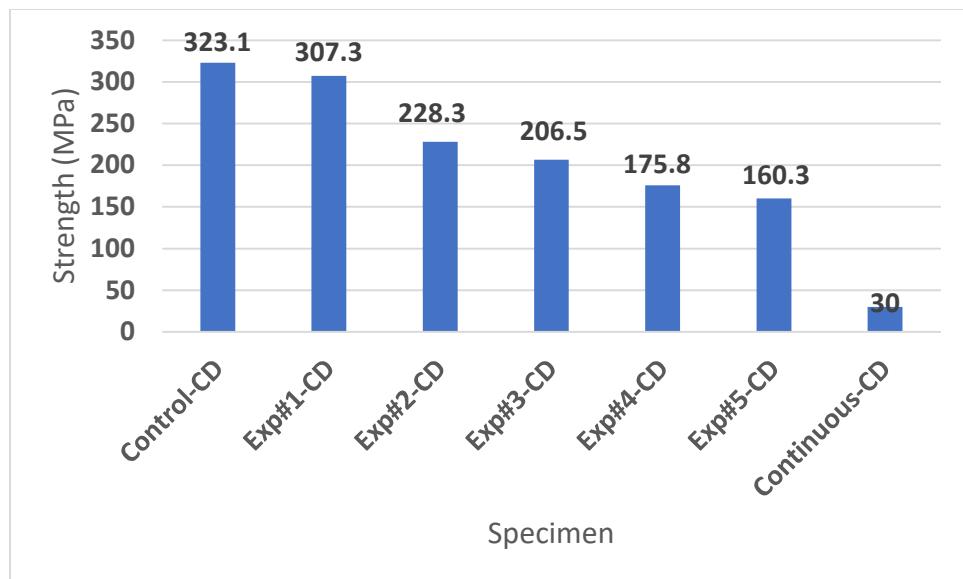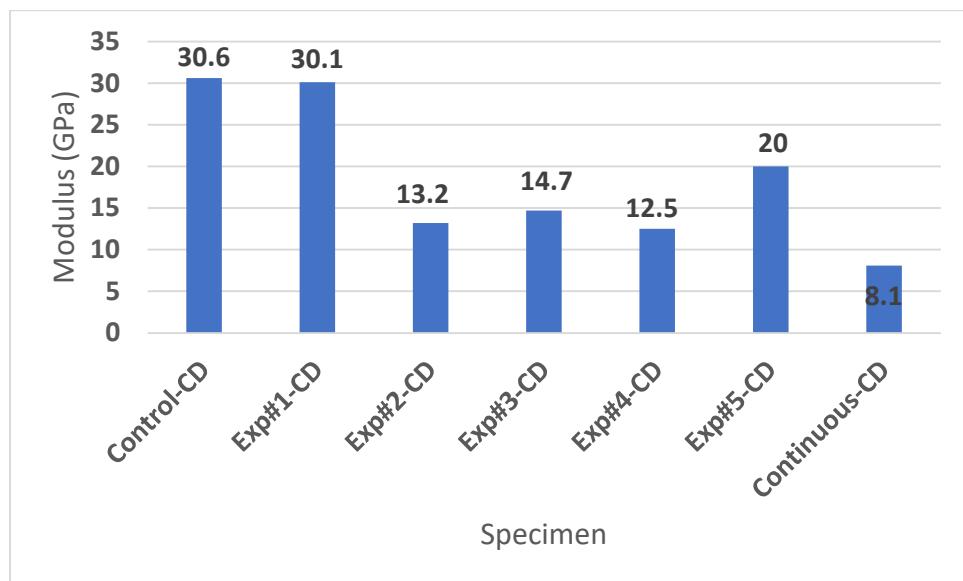
…..continued
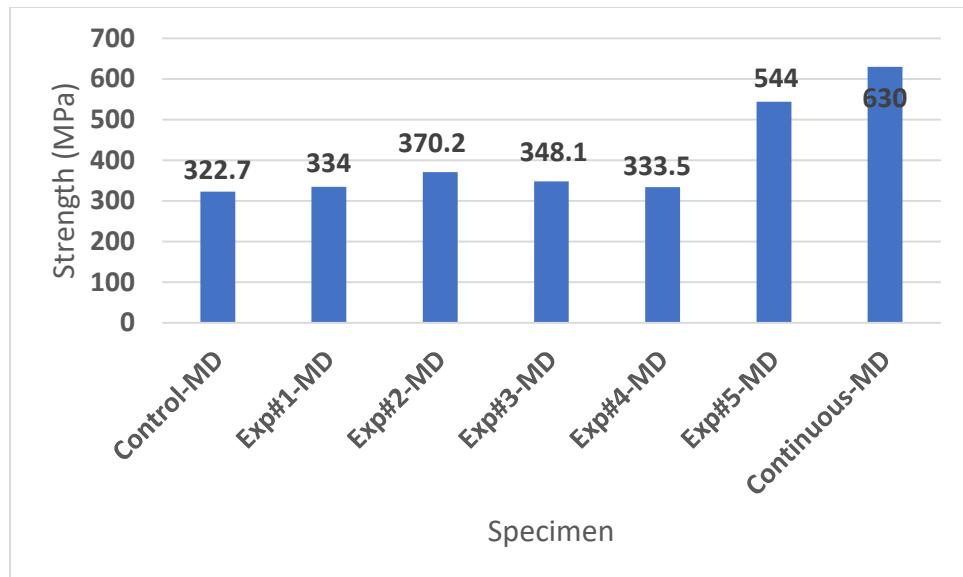
(c)
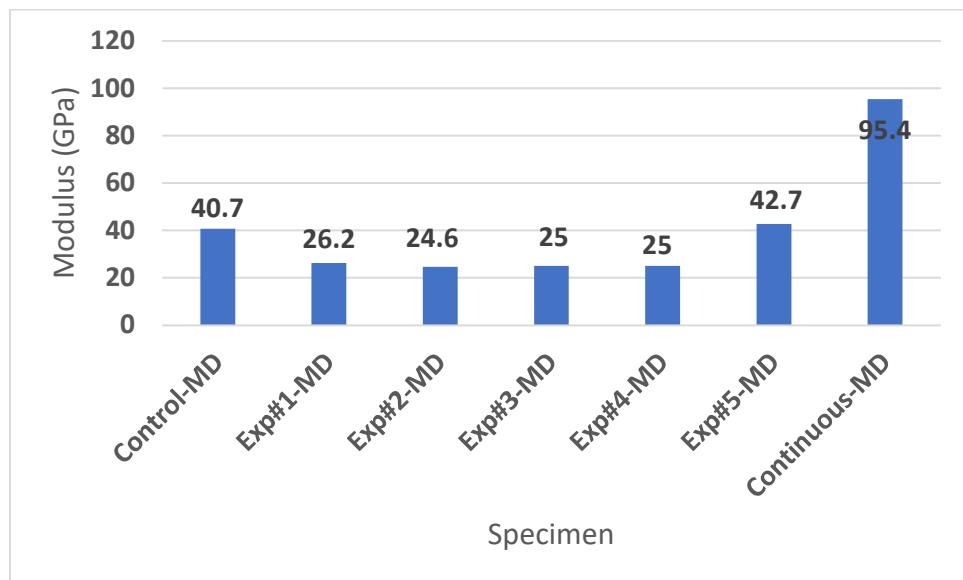
(d)

Figure 3. Comparative normalized data for flexural properties of composites from carbon fiber mats produced at various machine speeds. (a, b) strength and modulus for cross-direction; (c,d) strength and modulus for machine direction.

(a)

(b)

…continued

(c)

(d)

Figure 4. Comparative normalized data for tensile properties of composites from carbon fiber mats produced at various machine speeds. (a, b) strength and modulus for cross-direction; (c,d) strength and modulus for machine direction

(a)

(b)

….continued

(c)

(d)

Figure 4. Comparative normalized data for flexural properties of composites from carbon fiber mats produced at various basis weights. . (a, b) strength and modulus for cross-direction; (c,d) strength and modulus for machine direction.

(a)

(b)

(c)

(d)

Figure 5.Comparative normalized data for tensile properties of composites from carbon fiber mats produced at various basis weights. (a, b) strength and modulus for cross-direction; (c,d) strength and modulus for machine direction.
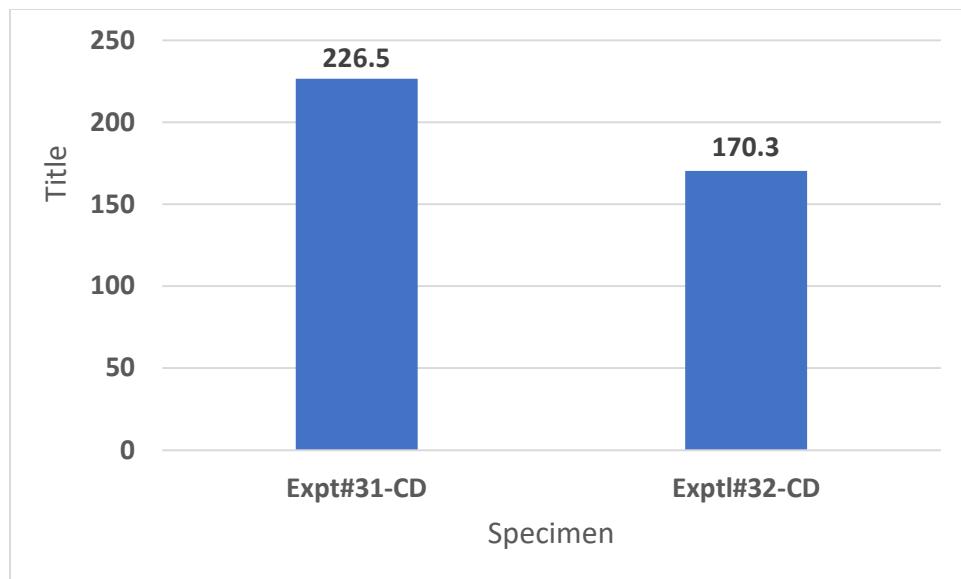
(a)
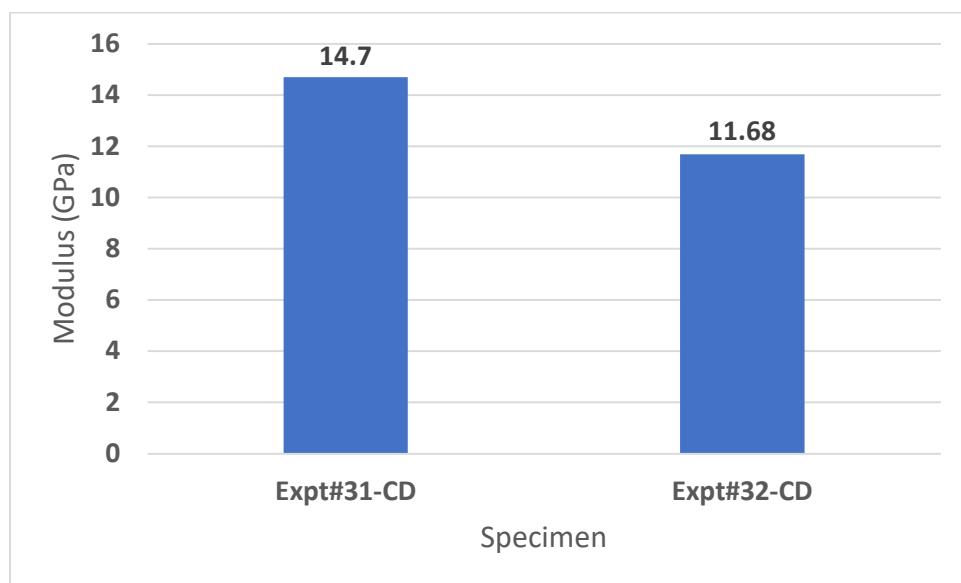
(b)
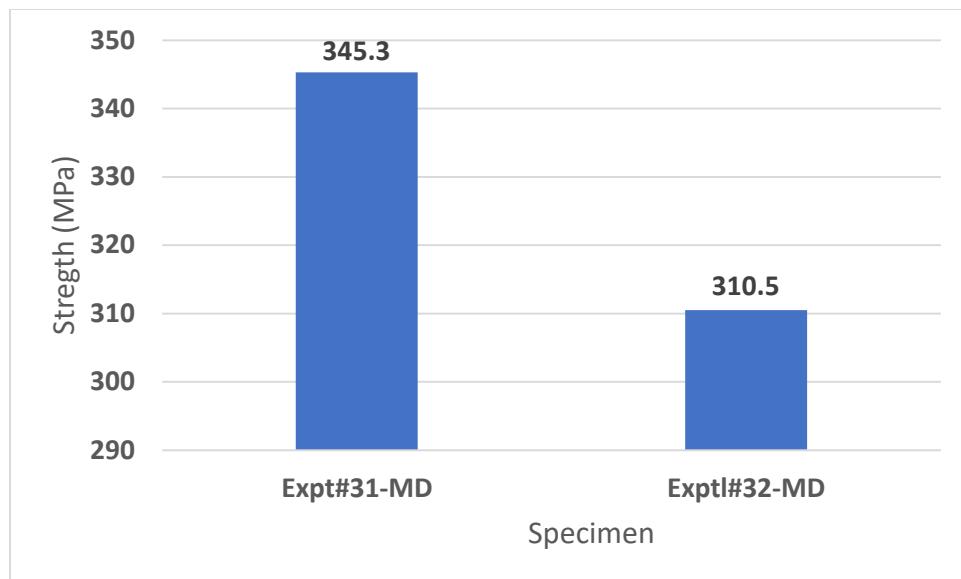
(c)
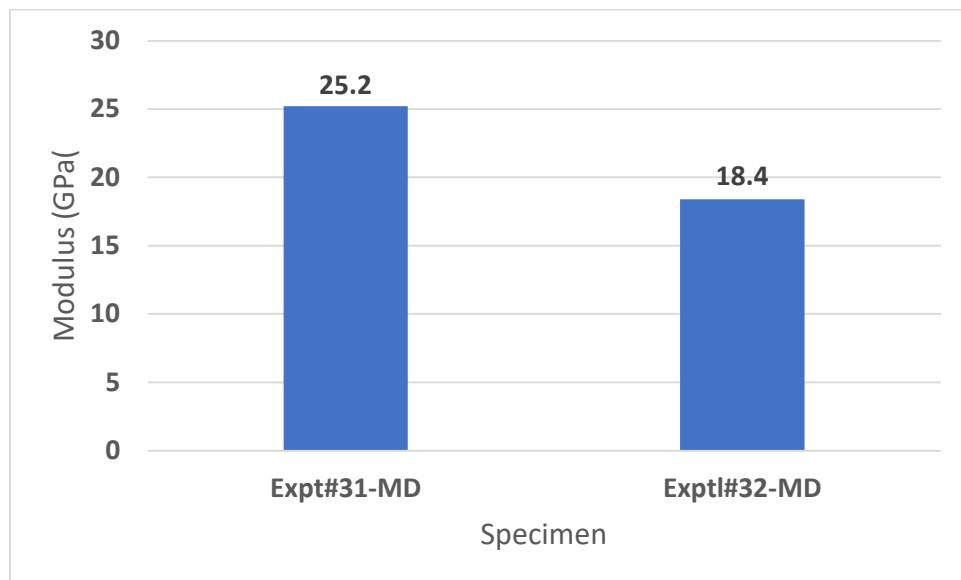
(d)

Figure 6.Comparative normalized data for flexural properties of composites from carbon fiber mats with varying fiber length. (a, b) strength and modulus for cross-direction; (c,d) strength and modulus for machine direction.
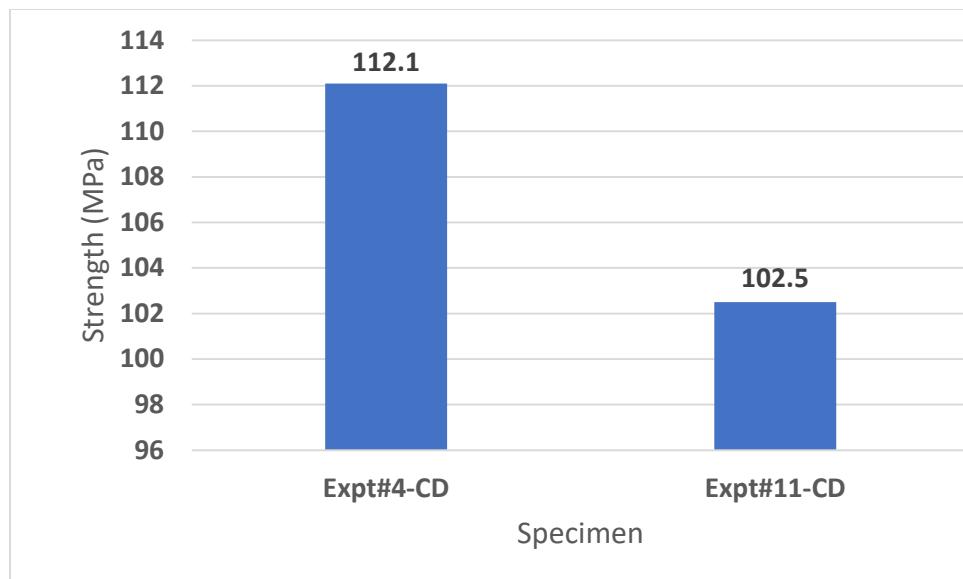
(a)
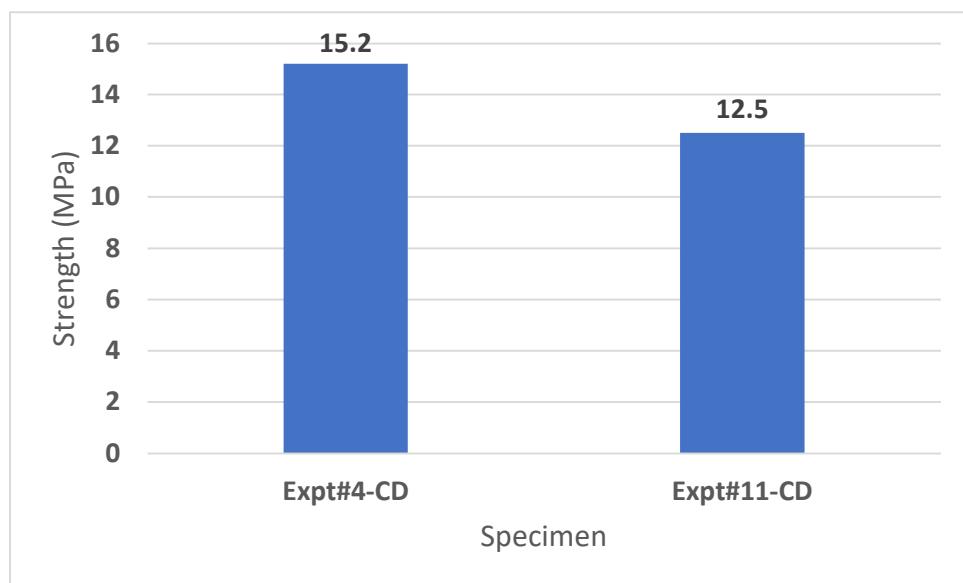
(b)
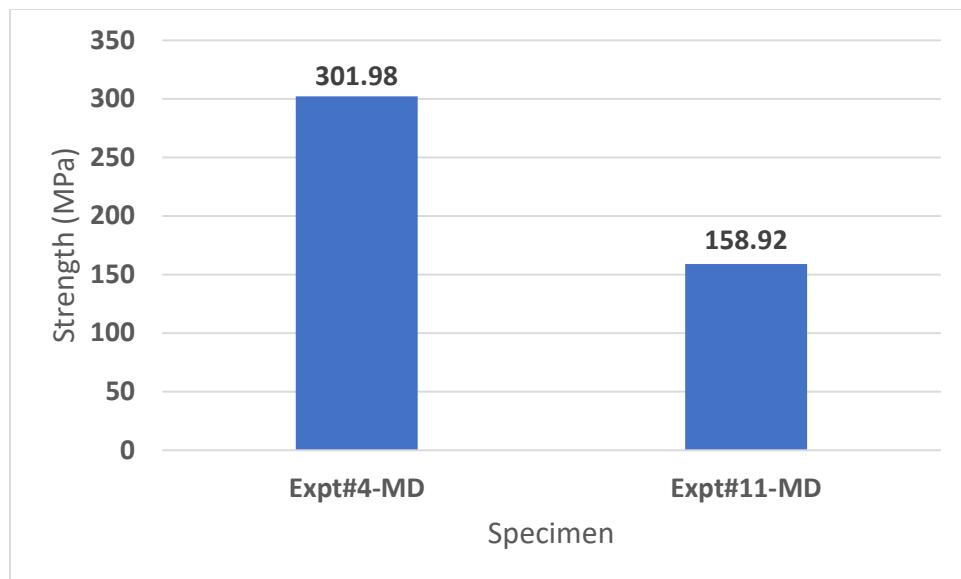
(c)
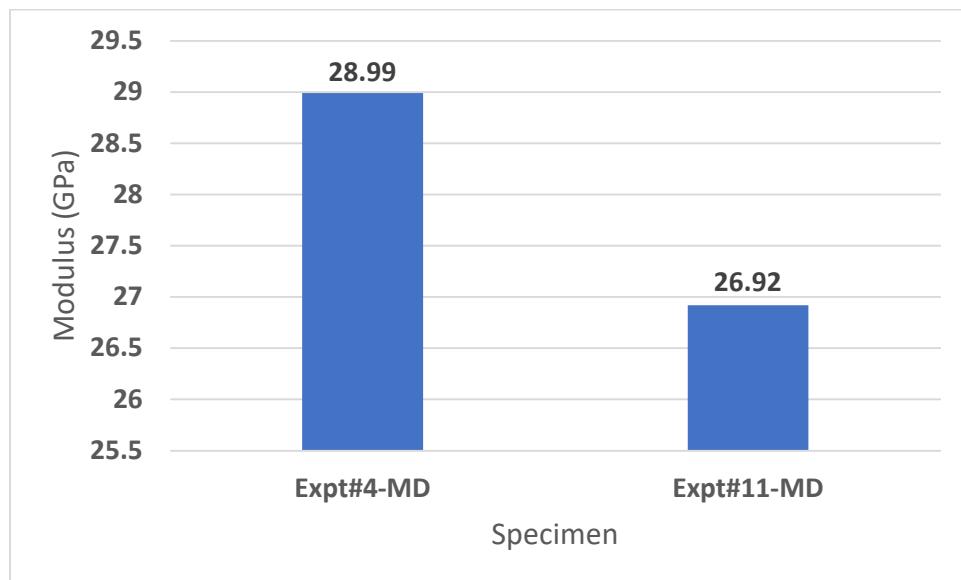
(d)

Figure 7. Comparative normalized data for tensile properties of composites from carbon fiber mats with varying fiber length. (a, b) strength and modulus for cross-direction; (c,d) strength and modulus for machine direction.
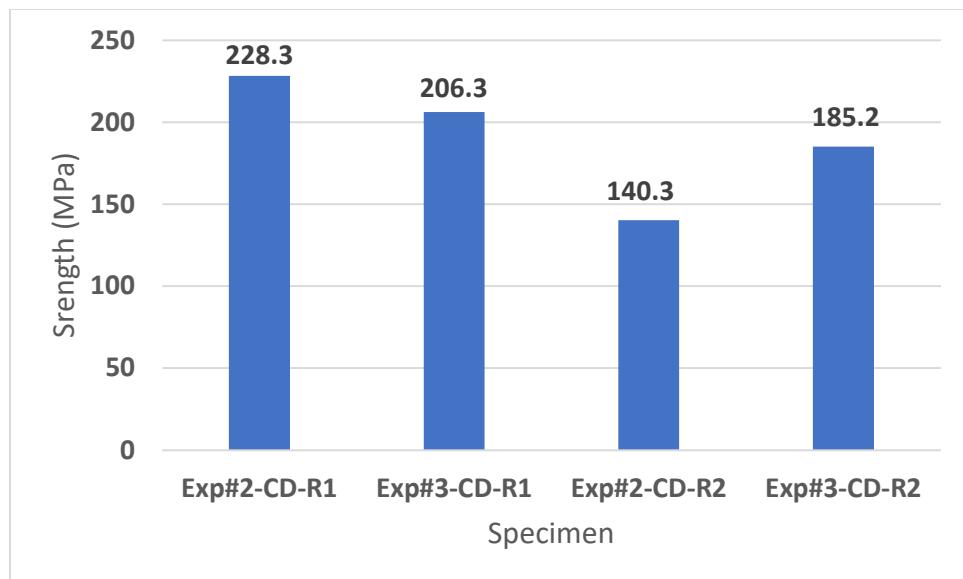
(a)
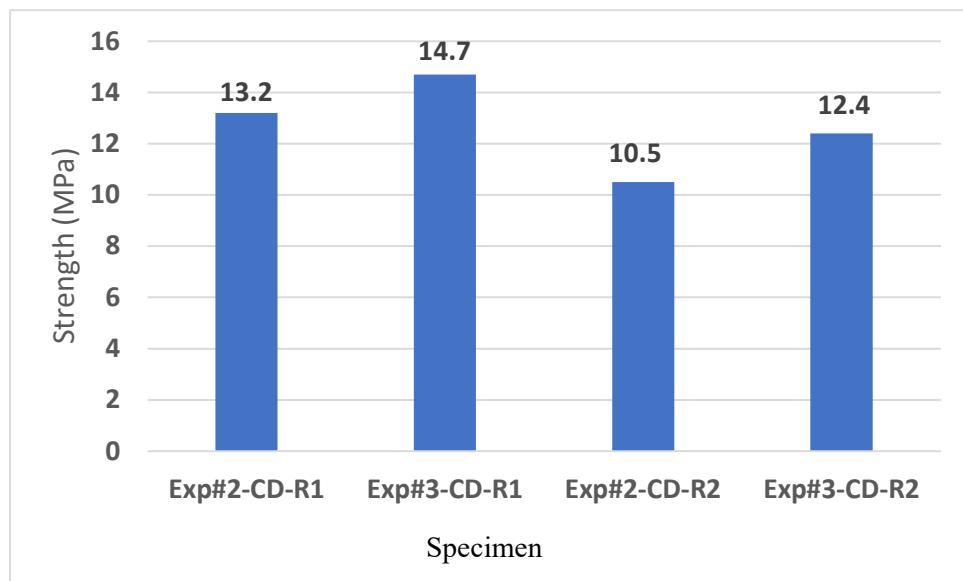
(b)
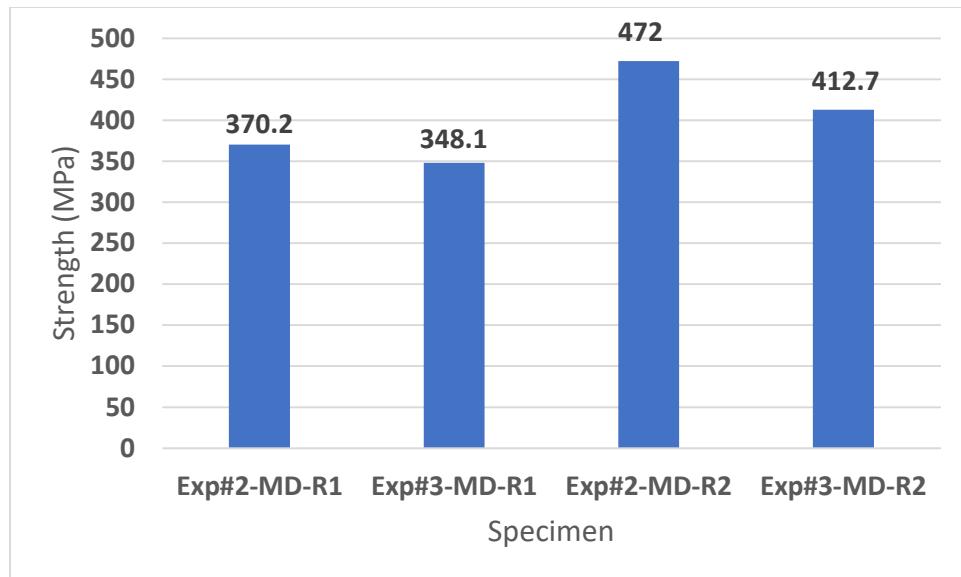
(c)
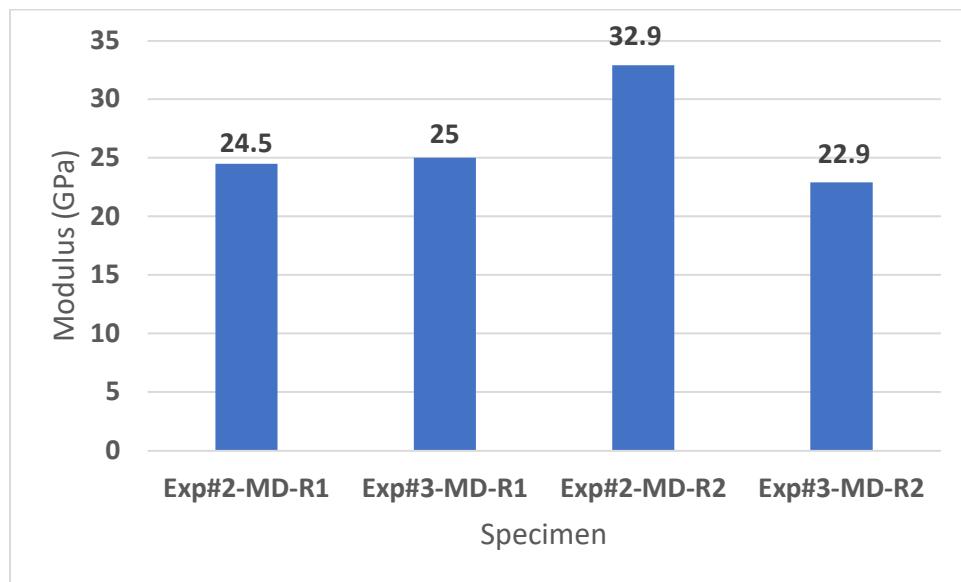
(d)

Figure 8. Comparative normalized data for flexural properties of composites from carbon fiber mats from two different batches. (a, b) strength and modulus for cross-direction; (c,d) strength and modulus for machine direction.
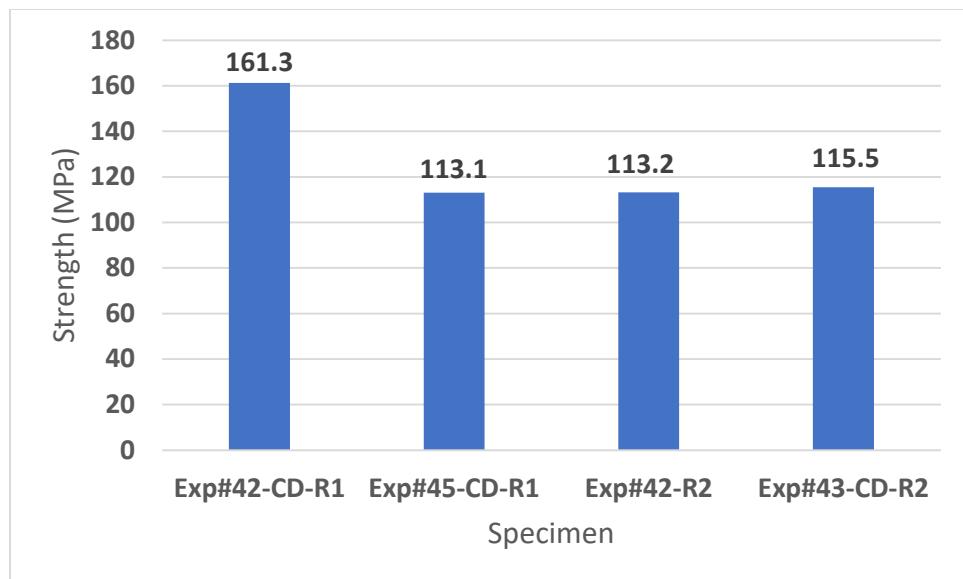
(a)
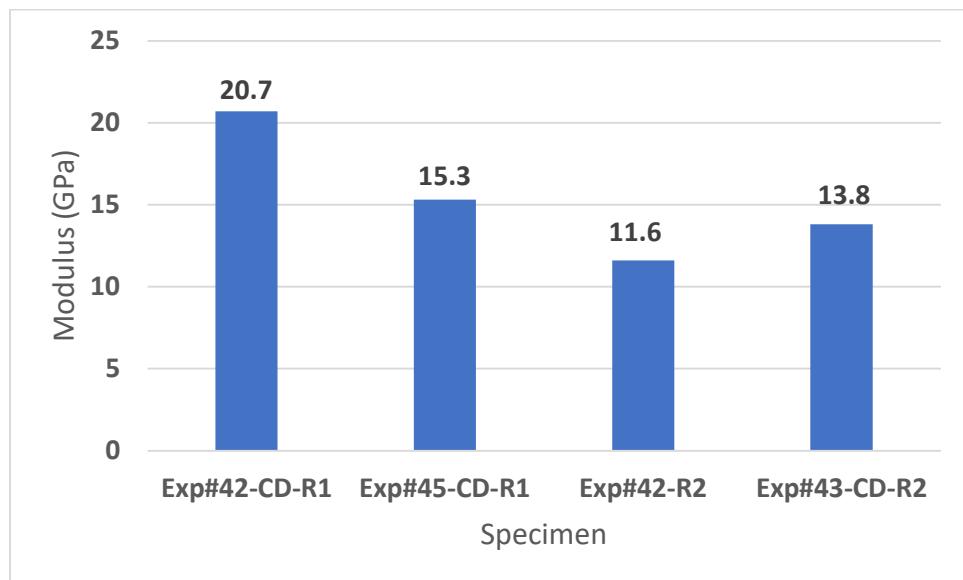
(b)
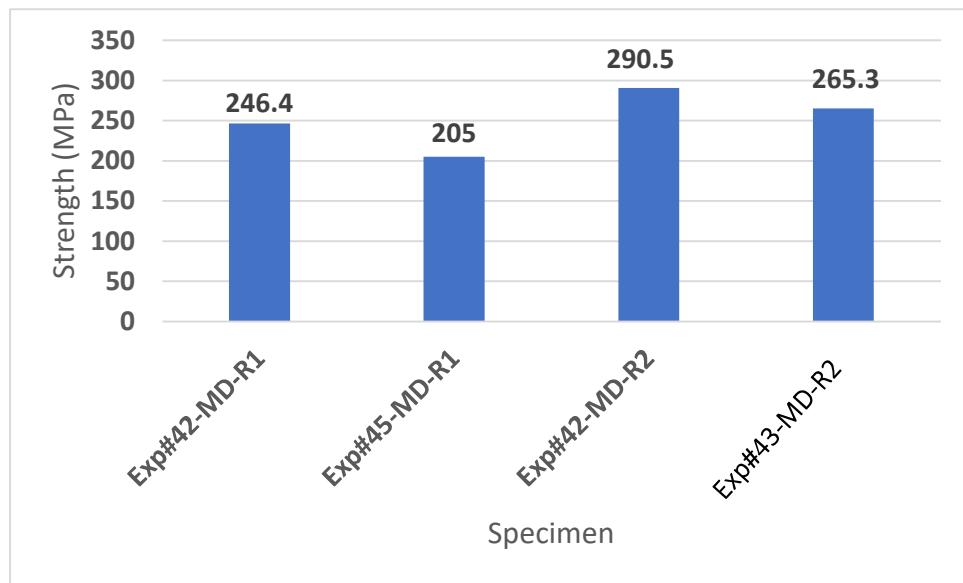
(c)
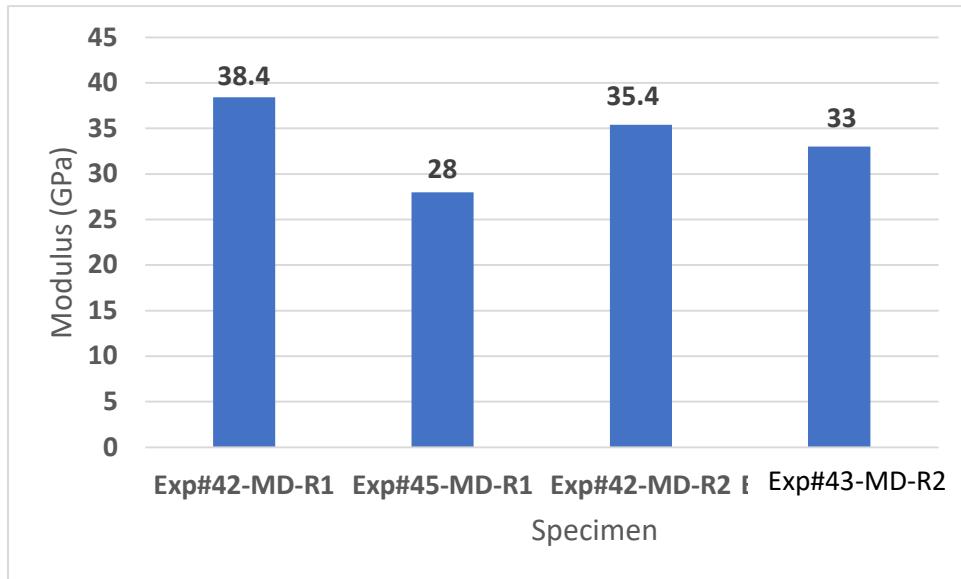
(d)

Figure 9. Comparative normalized data for tensile properties of composites from carbon fiber mats from two different batches. (a, b) strength and modulus for cross-direction; (c,d) strength and modulus for machine direction.
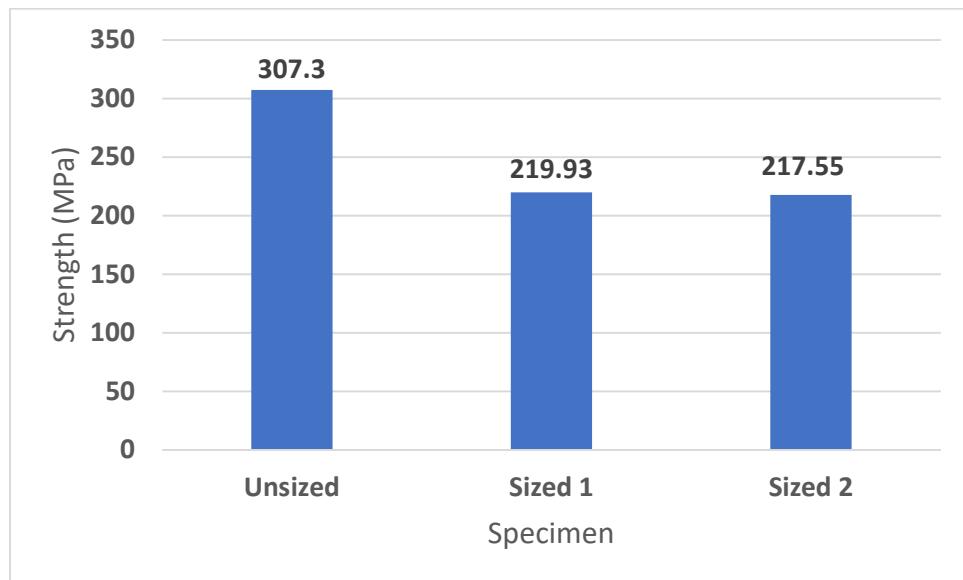
(a)
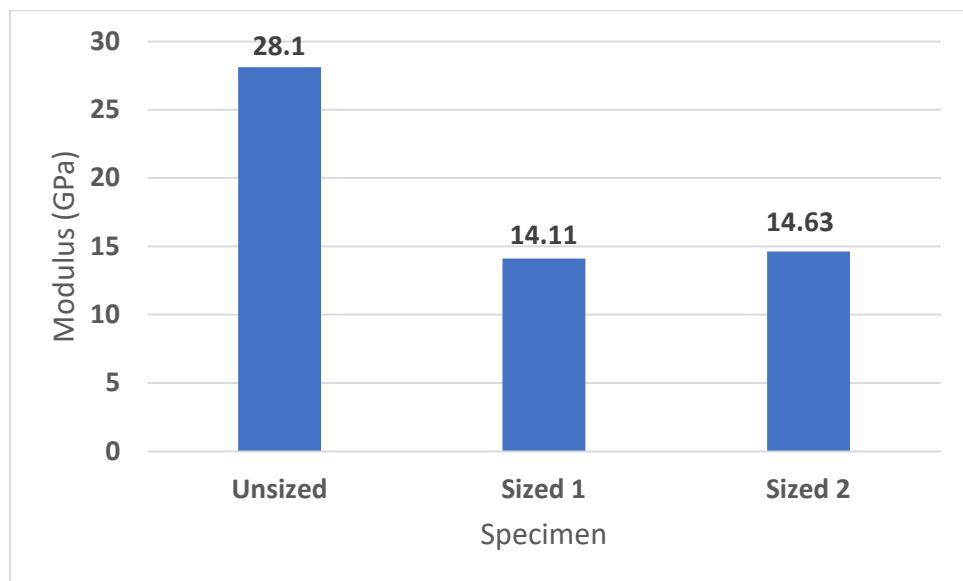
(b)
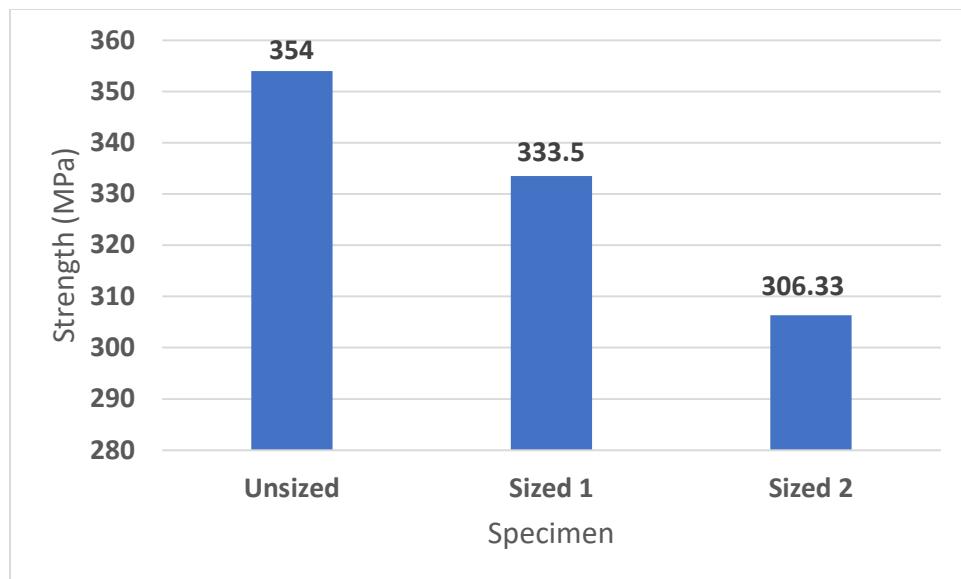
(c)
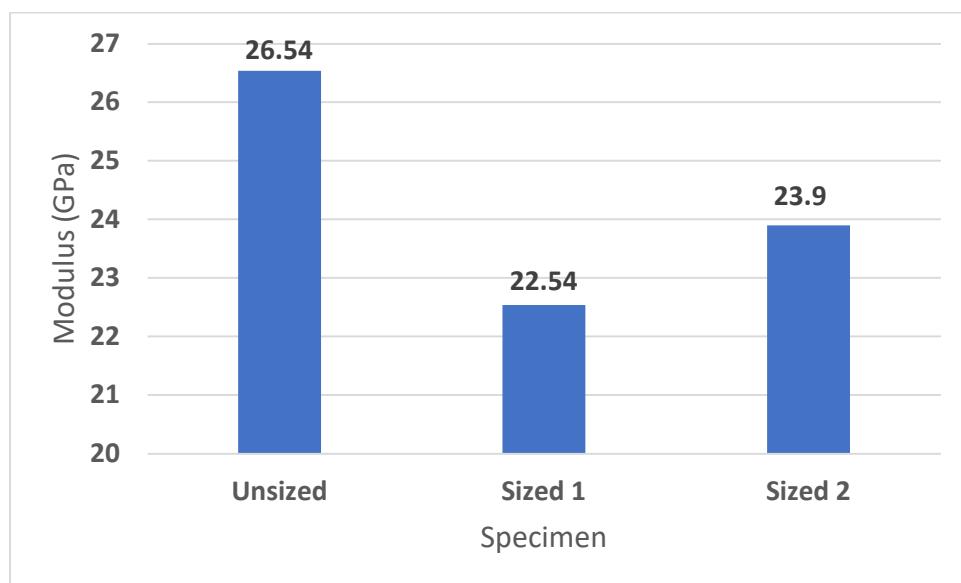
(d)

Figure 10.Comparative normalized data for flexural properties of composites from sizing study ,
(a, b) strength and modulus for cross-direction; (c,d) strength and modulus for machine direction.
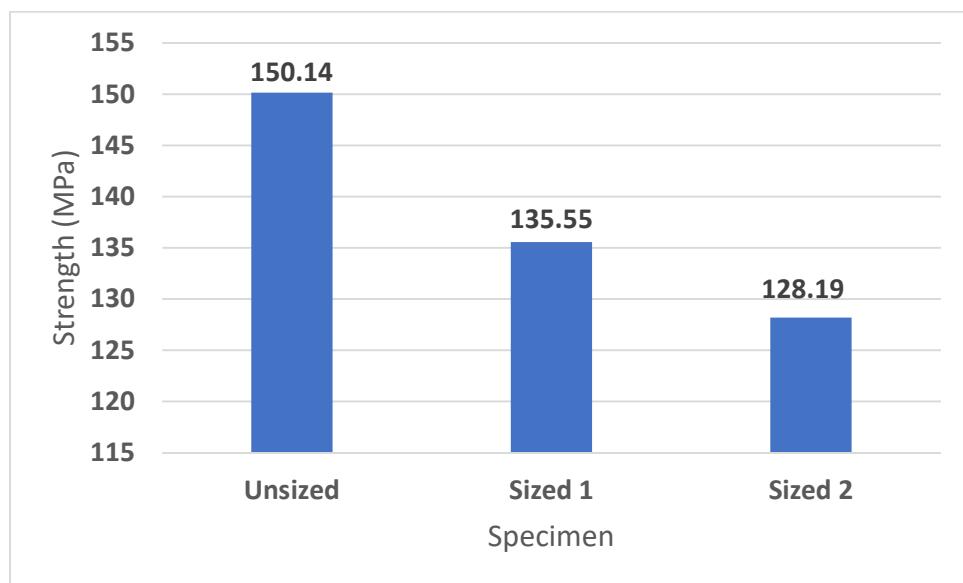
(a)
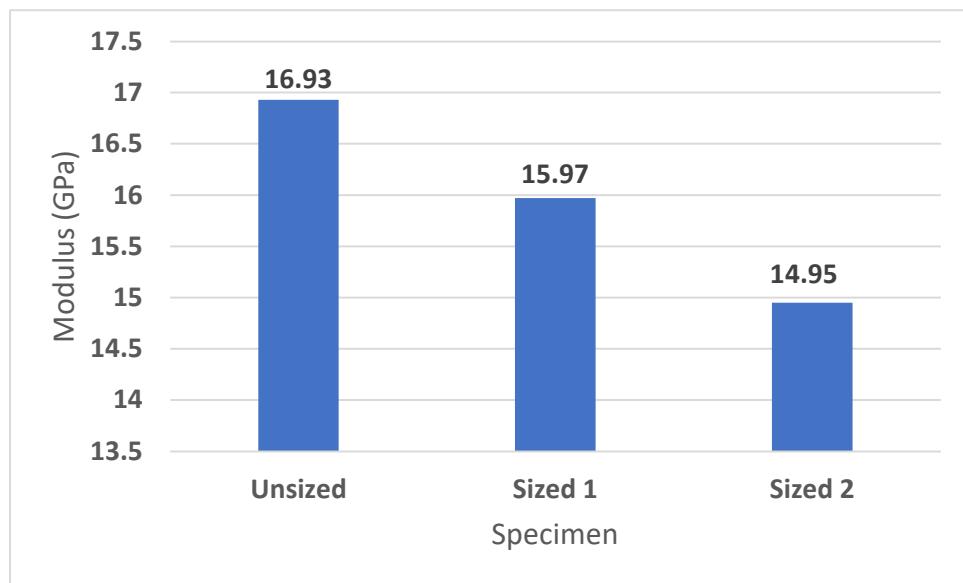
(b)
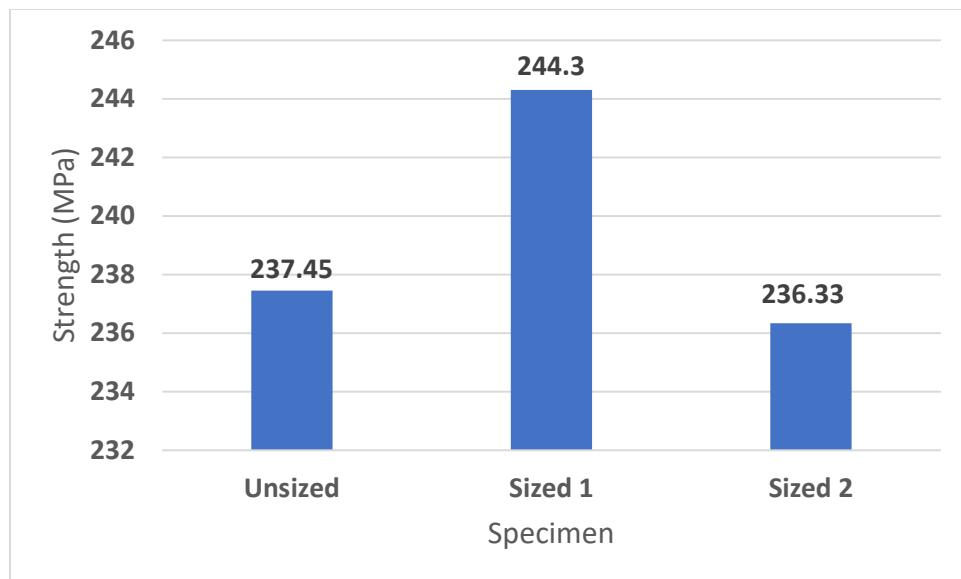
(c)
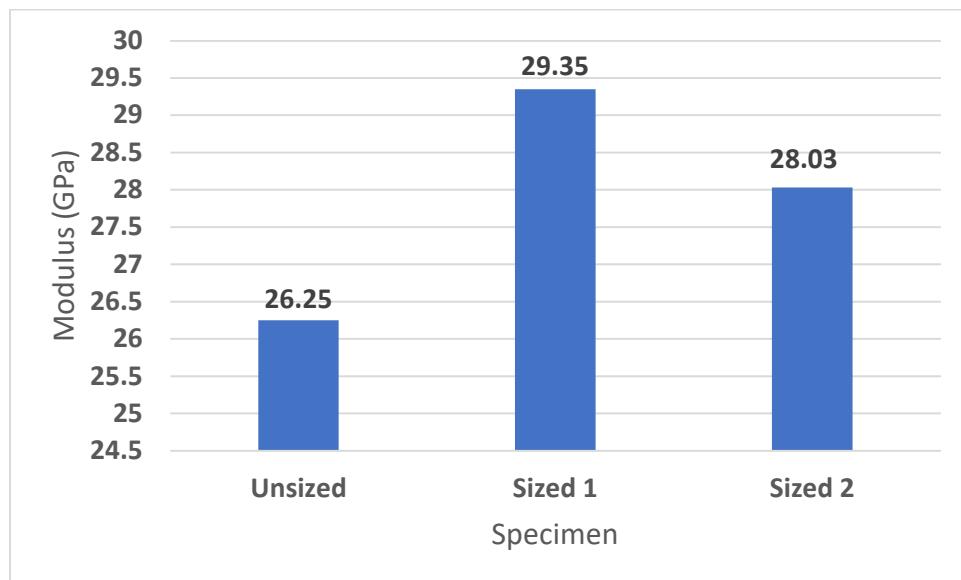

(d)

Figure 11.Comparative normalized data for tensile properties of composites from sizing study.
(a, b) strength and modulus for cross-direction; (c,d) strength and modulus for machine direction.

## 5.7 Fiber orientation characterization versus mechanical performance study

A key goal of this study was to evaluate the aligned mats unidirectional mechanical properties in the fabricated carbon fiber mats. It was hypothesized that the discontinuous aligned fibers would have intermediate properties between isotropic SMCs and continuous unidirectional prepreg. To that end, the orientation of the fibers within a nonwoven preform is a critical factor in the mechanical properties of any final composite. While slow methods exist for accurately measuring fiber orientation on small scale, industry needs fast methods for analyzing fiber orientation distribution in large area samples and easy correlation with final mechanical properties for commercial scale production.

An analytical model for fast fiber orientation analysis was built using Krenchel's modified Voigt estimate (i.e., modified rule of mixtures) for fiber reinforced composite Young's modulus with complex fiber orientation distributions. Krenchel's relation is as follows:

$$E_c = \eta_{KOF}\eta_{KLE}E_f V_f + E_m V_m,$$

where E_c is composite Young's modulus, η_{KOF} is Krenchel's orientation factor (KOF), η_{KLE} is Krenchel's length efficiency factor (KLE), E_f is fiber phase modulus, E_m is matrix phase modulus, V_f is fiber phase volume fraction, and V_m is matrix phase volume fraction. That is η_{KOF} and η_{KLE} are used to modify the theoretical strength of a continuous fiber composite to account for both fiber discontinuity and arbitrary orientation distributions. The value of η_{KOF} varies between unity (100% of fibers at 0° to measured direction) and null (100% of fibers at 90° to measured direction).

An advantage of this approach is that it provides a simple scalar indicator by which different, complex fiber orientation distributions can be compared against one another in terms of predicted/measured composite mechanical performance. While theory can overestimate real composite performance by not accounting for material defects (e.g., voids) that will inevitably reduce final properties, the model is expected to be relatively close for modulus calculations as tensile elastic behavior is less sensitive than strength to such defects. η_{KOF} is calculated from fiber orientation distribution through the following relation:

$$\eta_{KOF} = \sum_n a_n \cos^4 \phi_n$$

where n is fiber orientation direction index, ϕ_n is fiber angle from 0° reference direction, and a_n is the fraction of fibers at orientation ϕ_n. For example, in a perfectly isotropic reinforced composite fiber will be on average be aligned such that $a_1 = a_2 = a_3 = a_4 = 0.25$ for $\phi_1 = 0°$, $\phi_2 = 45°$, $\phi_3 = 90°$, $\phi_4 = -45°$ yielding $\eta_{KOF} = 0.375$. η_{KLE} is calculated using the following relation:

$$\eta_{KLE} = 1 - 2(l_c/l)$$

where l is embedded fiber length and l_c is the critical fiber length which determines whether a fiber or its surface interface with the composite matrix fails first during loading. Using an assumed

nominal l_c of 1mm, $\eta_{KLE} = 0.833$ for the 12mm fibers used in most of the fabricated mats. With the Krenchel model in place, η_{KOF} values backcalculated from mechanical properties data can be compared against forward calculated fiber orientation measurements to validate and confirm the measured distributions. Tables 1 and 2 show measured Young's modulus back calculated η_{KOF} values for both the mats produced by Neenah in their initial February trial runs and their later August main trial runs, respectively. The Expt#2 August 2018 trial and its February 2019 equivalent run η_{KOF} values closely matched. Expt#3 August 2018 run sample η_{KOF} value appears lower than its February equivalent. Expt#5, the highest production speed sample, achieved the highest η_{KOF}. This represents fiber alignment distribution that is ~52% compared to 0° and ~48% compared to 90° aligned fiber composite. Furthermore, the hand sheet wet laid isotropic mats, increased fiber length, and increased fiber gsm exhibited lower η_{KOF} than the production samples.

Most other conditions however were around or below the expected performance of an isotropic mat, 0.375. In terms of composite output tensile modulus (GPa)/CF reinforcement (vol%); Expt#1 (isotropic), 0.71 < Expt#5 (high speed aligned), 1.12 < Continuous fiber composite, 2.13; showing a clear enhancement in CF reinforcement efficiency of the aligned nonwoven.

Table 1. Measured composite parameters and back calculated η_{KOF} after epoxy infusion and compression molding of the nonwovens produced during the February 2019 trial runs

Specimen	Fiber volume %	Measured E (GPa)	KOF
C-50	34%	30.1	0.412
C-100	38%	31.3	0.386

Table 2. Measured composite parameters and back calculated η_{KOF} after epoxy infusion and compression molding of the nonwovens produced during the August trial runs. August 2018 trials KOF calculations

Specimen	Fiber volume %	Measured E (GPa)	KOF
C-50 (Expt#2)	31%	28.2	0.420
C-100 (Expt#3)	34%	24.6	0.331
C-200 (Expt#4)	42%	33.7	0.379
C-300 (Expt # 5)	30%	33.5	0.522

Isotropic Expt # 1	31%	21.9	0.319
1 gsm (Expt 7-1)	42%	26.9	0.298
Length (Expt # 11)	39%	25.6	0.304

To begin direct capture of the fiber orientation distribution in the nonwoven preforms, a Keyence digital microscope was used to capture the CF mat surface. Initial mat surface observation indicated a potential problem in using visual characterization as the example mat top and bottom surfaces in Fig. 13 clearly do not match. However, further observation of mat cross-sections in Fig. 14 indicated that the mats possessed layers from which the alignment can be interpreted.
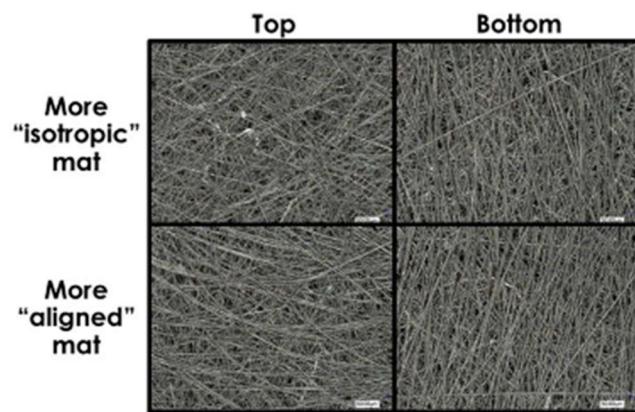
Figure 12. Top and bottom nonwoven mat surface fibers imaged with a Keyence Digital Microscope
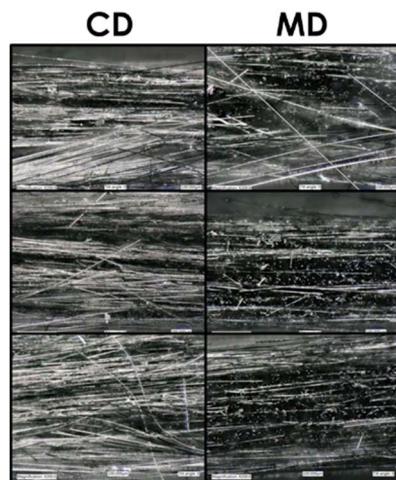
Figure 13. Nonwoven mat cross-section images of cross-direction (CD) and machine-direction (MD) proceeding in the top row to bottom as: Expt#2 (C-50), Expt#3 (C-100), Expt#5 (C-300) taken from the February 2019 runs.

Due to the dense, interconnected fiber network present in the optical images, they could not be readily segmented, and a threshold established for computer processing of fiber orientation. Overall image orientation though, which must directly correlate with fiber orientation, can be calculated by measuring the orientation of image greyscale values. FIJI/ImageJ's "Directionality" plug-in was selected to quantify alignment distribution in the nonwoven optical micrographs. To assess algorithm effectiveness, fiber alignment was imaged on a randomly selected sample region in Fig. 14 and quantified both manually and by machine. The algorithm appears to do a good job capturing the fiber orientation based on the distribution plot in Fig. 15. From Table 3, the computer fiber orientation distribution results agree to within a few degrees of the manual (human) fiber orientation measurement suggesting that the computer algorithm does an accurate job capturing the visible fiber orientation data.
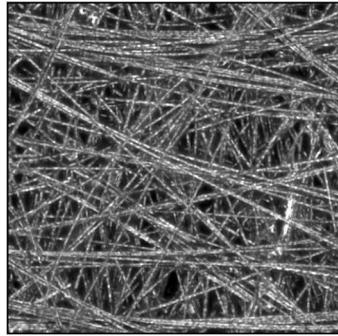
Figure 14. Image of August 2018 trials Exp#3 (C-100) sample surface used for alignment results comparison; image represents 1x1mm area which corresponds with the resolution of later eddy current measurements.
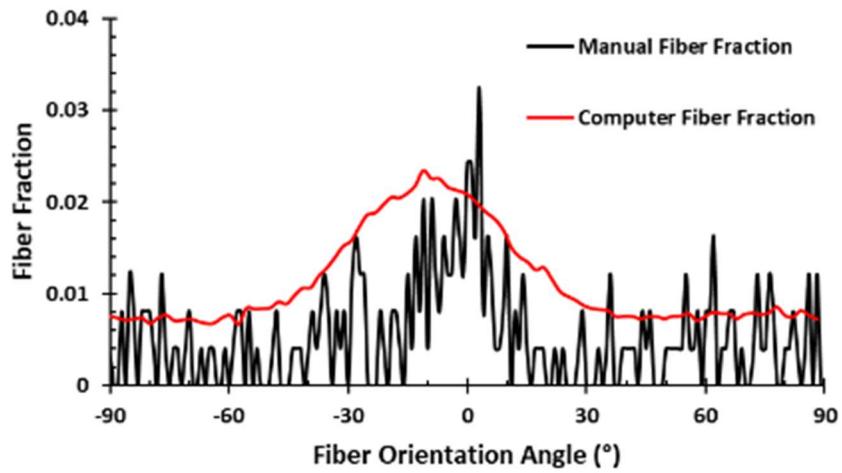
Figure 15. FIJI/ImageJ "Directionality" algorithm appears to do a qualitatively good job capturing the fiber orientation when compared to human measured fiber orientation distribution present in Fig. 15.

Table 3. Summary of fiber orientation distribution statistics based on Fig. 13 as measured via FIJI/ImageJ "Directionality" plugin and by human manual measurement.

Fiber Angle Results		
###	Human	Computer
Avg. Angle	0.42°	-3.15°
Std. Dev.	45.92°	43.82°
KOF	0.52	0.52

Computer analysis was then used to capture relative alignment of the nonwoven mat top and bottom surfaces. For the example surfaces characterized in Fig. 17., Table 4 results indicate one surface to be relatively aligned parallel with the production machine direction and the other relatively aligned perpendicularly. Assuming the mat to consist of even layers of these two structures, an average value $\eta_{KOF} = 0.411$ can be calculated.
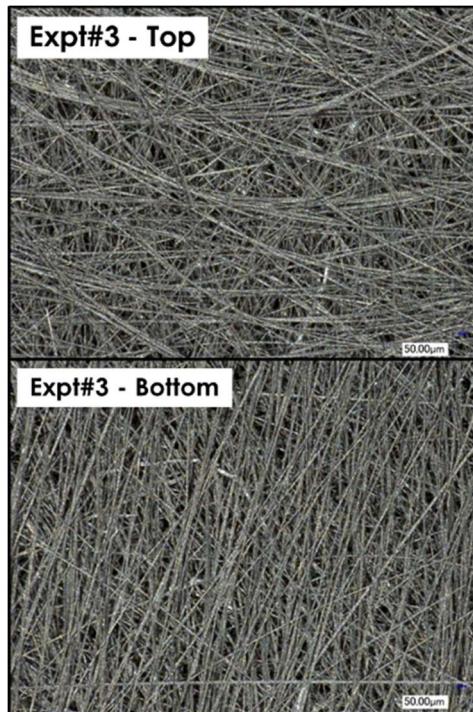
Figure 16.Optical micrographs of Expt#3 nonwoven surfaces for fiber alignment analysis.

Table 4. FIJI/ImageJ "Directionality" plugin calculated fiber orientation statistics for Expt#3 shown in Fig. 15.

For further comparison against the mechanical property back calculated and optical micrograph forward calculated η_{KOF}, fiber orientation measurements were conducted using eddy current measurements averaging local spot fiber orientations across mat thickness. Measurements were conducted using a Suragus Instruments EddyCus CF map 5050iso device which works by using 4 eddy current sensors oriented at $0°, 45°, 90°, 135°$ angles and computing strength of CF orientation along these cardinal directions based on directional conductivity strength. These are discussed in Figures 22 to 26. The full report, including sample heat maps of average fiber orientation, local anisotropy, and relative fiber areal weight, is available from Figure 22 to 26. By assuming that the sensor measured amount of conductive material is directly proportional to oriented fiber areal weight, average relative fiber fraction oriented along each sensor's direction was calculated along with sample η_{KOF}. This process was conducted on each starting nonwoven preforms and preforms after resin infusion and compression molding. The eddy current measured η_{KOF} values are compiled along side the mechanical and optical results in Table 5.

Expt#5's peak result in η_{KOF} appears to sit roughly halfway between isotropic and continuous results supporting a +50% relative fiber alignment. Optical and eddy current KOF values from the Expt#3 mats match closely but are noticeably above the corresponding mechanical results. In fact, all forward calculated η_{KOF} values are at least somewhat higher than their back calculated counterparts, as would be expected given the model's inability to compensate for material defects, although most still agree to with ~10%. Perhaps more interesting, however, is that eddy current measurements consistently showed higher η_{KOF} values after resin infusion and compression molding suggesting the possibility that the preferential fiber orientation imparted during the nonwoven production causes composite flow during later manufacturing processes to favor/reinforce the already preferred fiber orientation. However, more research would be needed to isolate out other potential influencing factors such as compression of the molded composites versus the loose nonwoven fiber-only mats.

Table 5.Summary of forward calculated (optical and eddy current) and back calculated (mechanical) η_{KOF} values for the various tested nonwoven mat fabrication conditions.

KOF Results Sorting

ID	SAMP	Mechanical		Optical	Eddy	Eddy-Inf
		Feb	Aug			
		KOF	KOF	KOF	KOF	KOF
UTK	Cont	xxx	0.862			
C-300	Exp#5	xxx	0.522	0.581[#]		
C-50	Exp#2	0.412	0.42			
C-200	Exp#4	xxx	0.379			
C-100	Exp#3	0.386	0.331	0.411[+]	0.416[*]	0.551
ISO	Exp#1	xxx	0.319	0.346[++]	0.346[++]	0.397
+ gsm	Exp#7-1	xxx	0.298			
+ length	Exp#11	xxx	0.304			

[#]KOF after 90° image rotation (i.e. CD) is 0.201.
[*]Measurement listed is for Aug. trial mat sample; Feb. trial mat was also measured at 0.424.
[+]KOF after 90° image rotation (i.e. CD) is 0.365.
[++]Optical KOF in table is CD to match orientation Suragus measured. KOF before 90° image rotation is 0.422.

5.8 Other nonwoven mat characterization data

During optical characterization of fiber orientation in the nonwovens, bulges in the mat bottoms were observed that became more pronounced at higher speeds. Imaging the bulges revealed noticeably more residue, which looks like binder, present at the bump locations versus background mat as shown in Fig. 18. This data suggests a potential correlation with the binding agent used in mat production and the observed mat defects. However, the residue could also be some other form of debris interfering with the wet laidprocess.
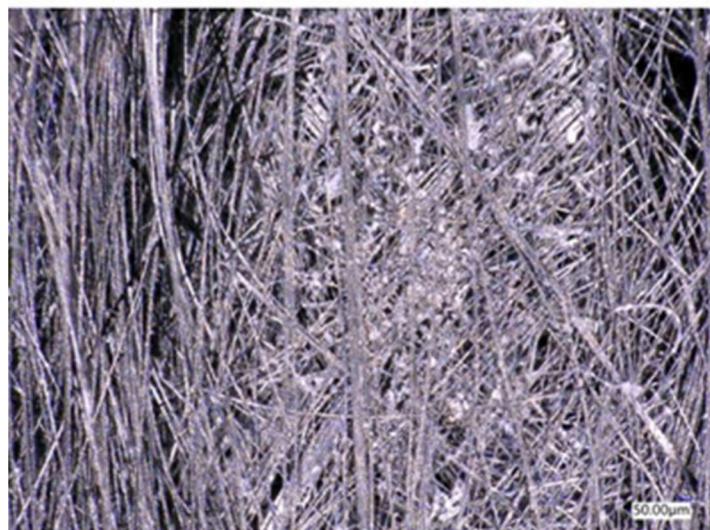
Figure 17.Picture of Expt#5 (C-300) sample bottom surface with bumps with optical micrograph zoom in revealing presence of residue substance does not present in the flat regions of the mat.

One of the questions that emerged as the project progressed was to explore increasing oxygen content on the fiber surface such that the CF mats would contain > 7% atomic oxygen to carbon ratio on the carbon fiber surface. To give the fibers better bonding properties, their surface is slightly oxidized. The addition of oxygen atoms to the surface provides better chemical bonding properties and etches and roughens the surface for better mechanical bonding properties. This was accomplished using an indirect, elevated temperature, continuous plasma treatment process. Mats were plasma processed in pure oxygen, elevated oxygen, and ambient atmosphere and then the surface chemistry measured via XPS. The full results of these tests are summarized in Fig. 19 and 20.

Additional details and the feasibility study for fiber orientation are provided in Appendix A.

Plasma Surface Treatment - 1

- Plasma treatment type: Indirect exposure
- Process gas: oxygen
- Treatment time: 15 min
- Temperature: elevated but <200°C
- Process Type: continuous

Sample 3A Example Data

Area 3

Area 2

Area 1

1200   1000   800   600   400   200   0
Binding Energy (eV)
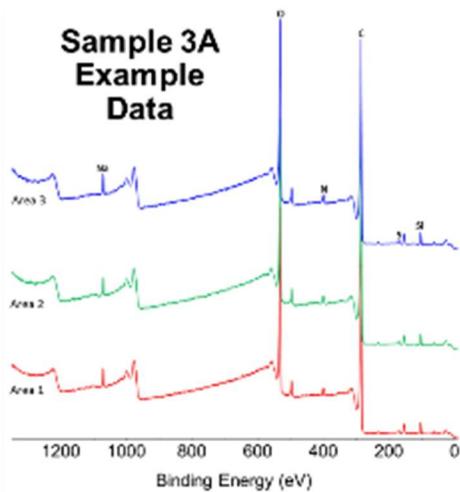
Surface Samples

Surface Composition (at.%) - 3A

	C	O	N	Si	Na	S
Area 1	66.3	27.1	1.8	3.2	1.2	0.5
Area 2	67.6	26.1	1.7	2.9	1.2	0.5
Area 3	67.0	26.4	1.7	3.0	1.4	0.5
Average	67.0	26.5	1.8	3.0	1.3	0.5

Surface Composition (at.%) - 3B

	C	O	N	Si	Na	S
Area 1	65.8	27.4	1.7	3.1	1.5	0.6
Area 2	67.7	25.5	1.7	2.9	1.5	0.7
Area 3	66.2	26.2	1.9	3.6	1.5	0.7
Average	66.6	26.4	1.8	3.2	1.5	0.6

Surface Composition (at.%) - 3C

	C	O	N	Si	Na	S
Area 1	68.3	25.4	1.6	2.6	1.6	0.6
Area 2	67.0	25.9	1.8	2.9	1.7	0.7
Area 3	67.0	25.9	1.7	3.0	1.7	0.7
Average	67.4	25.7	1.7	2.8	1.7	0.7

Core Samples

Surface Composition (at.%) - 3D

	C	O	N	Si	Na	S
Area 1	67.8	26.4	1.7	2.3	1.4	0.4
Area 2	68.9	26.2	1.5	1.8	1.3	0.4
Area 3	67.9	25.6	1.7	2.7	1.5	0.6
Average	68.2	26.1	1.6	2.2	1.4	0.5

Surface Composition (at.%) - 3E

	C	O	N	Si	Na	S
Area 1	65.7	27.1	1.7	2.8	1.9	0.8
Area 2	66.9	27.6	1.5	2.1	1.4	0.4
Area 3	66.9	27.4	1.4	1.9	1.7	0.6
Average	66.5	27.4	1.6	2.3	1.7	0.6

Surface Composition (at.%) - 3F

	C	O	N	Si	Na	S
Area 1	68.4	26.3	1.5	2.0	1.5	0.5
Area 2	67.3	25.9	1.8	2.7	1.6	0.7
Area 3	69.0	26.3	1.5	1.7	1.3	0.4
Average	68.2	26.2	1.6	2.1	1.4	0.5

Figure 18.Nonwoven mats plasma processed in pure oxygen with 3 samples processed pure condition; XPS samples taken from the mat surfaces and interior core regions for chemical analysis.

Plasma Surface Treatment - 2

- Plasma treatment type: Indirect exposure
- Process gas: oxygen enriched atmosphere vs. ambient
- Treatment time: 15 min
- Temperature: elevated but <200°C
- Process Type: continuous

Sample 3A Example Data

Binding Energy (eV)

Oxygen Enriched

Surface Composition (at.%) - 1A

	C	N	Na	O	S	Si
Area 1	71.9	1.7	1.0	24.7	0.3	0.5
Area 2	75.5	1.8	1.1	20.7	0.4	0.6
Area 3	77.1	2.2	1.2	18.6	0.4	0.5
Average	74.8	1.9	1.1	21.3	0.4	0.5

Surface Composition (at.%) - 1B

	C	N	Na	O	S	Si	Ca
Area 1	74.9	2.1	1.0	20.6	0.5	0.7	0.2
Area 2	77.2	1.9	1.0	18.7	0.4	0.5	0.3
Area 3	75.5	1.8	1.1	20.5	0.4	0.5	0.3
Average	75.9	1.9	1.0	19.9	0.4	0.6	0.3

Surface Composition (at.%) - 1C

	C	N	Na	O	S	Si	Ca
Area 1	74.6	1.9	1.1	21.4	0.4	0.5	0.1
Area 2	76.9	1.7	1.1	19.4	0.4	0.5	0.1
Area 3	79.0	2.1	0.9	16.9	0.3	0.6	0.2
Average	76.8	1.9	1.0	19.2	0.4	0.5	0.1

Ambient Atmosphere

Surface Composition (at.%) - 1D

	C	N	Na	O	S	Si
Area 1	78.0	2.0	1.7	17.3	0.6	0.6
Area 2	75.0	1.8	0.7	21.9	0.2	0.3
Area 3	77.5	1.9	1.1	18.7	0.4	0.5
Average	76.8	1.9	1.2	19.3	0.4	0.5

Surface Composition (at.%) - 1E

	C	N	Na	O	S	Si
Area 1	78.9	2.0	1.5	16.9	0.4	0.3
Area 2	75.9	1.7	1.3	20.4	0.4	0.4
Area 3	76.0	2.0	1.5	19.6	0.5	0.4
Average	76.9	1.9	1.4	19.0	0.4	0.4

Surface Composition (at.%) - 1F

	C	N	Na	O	S	Si
Area 1	78.2	2.0	1.0	18.2	0.2	0.4
Area 2	79.3	2.3	1.5	16.0	0.5	0.4
Area 3	77.6	1.7	1.4	18.6	0.4	0.4
Average	78.4	2.0	1.3	17.6	0.4	0.4

Figure 19.Nonwoven mats plasma processed in oxygen enriched and ambient atmospheres with 3 samples processed pure condition; XPS samples taken from the mat surfaces for chemical analysis.

6 BENEFITS ASSESSMENT

The key benefits of this technology are the reduced energy costs of multiple processes required to get alignment in the carbon fibers. These include high energy carding, resonant acoustic mixing, chemical agitation to name a few. By being able to produce alignment in-line in a process reduces overall energy costs.

The potential benefits that could be realized in downstream work is the extended fatigue life, higher performance, and high draw ratio achievable to create complex objects. The overall energy consumption can be reduced due to higher line speeds yielding higher aligned fibers. The collective composites conversion work through partnerships with UT, ORNL and industry partners can further enable product development.

7 COMMERCIALIZATION

During this project, Neenah Paper made some business decisions and decided to solely focus on paper products. The company decided to reevaluate the business strategies for discontinuous carbon fiber related intermediates. This timeline also coincided with Covid 19 which further affected many companies in their long-term investment plans. It can be said though that the outcome and results from this work has numerous outlets in synergistic IACMI projects. In discussion with IACMI, aligned discontinuous mats have applications in multi-material sheet molding compound (SMC), hybrid intermediates, over molding of continuous fiber with aligned discontinuous core to name a few. The time to develop future solutions will be greatly minimized as demonstrated by this work.

8 ACCOMPLISHMENTS

The project resulted in publications as follows:-

Uday Vaidya, Surbhi Kore, Ganesh Deka, Vidyarani Hiremath, Robert Conforti and Soydan Ozcan., Discontinuous carbon fiber processing and property bounds., Key Engineering Materials journal., Submitted to Journal of Engineered Fibers and Fabrics (In review).

Ryan Ginder, Ganesh Deka, Uday Vaidya., Characterization of discontinuous carbon fiber mats., Materials Evaluation., In preparation (May 20222).

Graduate students & thesis

- Surbhi Kore, PhD student, Fibers and Composites Manufacturing Facility, University of Tennessee
- Vidyarani Hiremath, MS, Fibers and Composites Manufacturing Facility, University of Tennessee

- Ryan Ginder, Post-doctoral fellow, UT and ORNL joint work

Undergraduate students' contribution to this project:- Vinit Chaudhary, Ryan Ogle, Jacob Williams, Patrick Cole and Eilish Stanik

9   CONCLUSIONS

The specific objective of this project was to produce a wet-laid nonwoven carbon fiber mat with a high degree of unidirectional fiber alignment, using discontinuous carbon fibers.

The project demonstrated that the aligned carbon fiber intermediates can be obtained up to line speeds of 300 ft/min, which is highly scalable. Remarkable improvements in tensile/flexural properties were not obtained due to some degree of randomness and emergence of surface imperfections between 200 to 300 ft/min for high fiber weight fractions. The line speed-alignment was more obtained for lower weight fractions < 20 weight%. However, valuable insights were gained on the feasibility of the process for carbon fibers.

While 100% alignment of carbon fiber was not realized, the microscopy data suggests that a majority portion > 70% did attain alignment up to ~ 300 ft/min. The effects of sizing remained partially studied and indicated that sizing has a strong influence on the surface of the wet laid mat and hence some limitations for alignment. This aspect needs further studies, which were beyond the scope of this work. We believe the work provided valuable path forward for future optimization efforts to realize commercial scale intermediates.

Conclusions from tests conducted with selected process parameters and starting material properties on carbon fiber mat intermediates and composites are as follows:-

Machine speed: The effect of machine speed during mat production is the first parameter considered for mechanical property evaluation. Mechanical properties of panels from mats produced from various machine speeds i.e., 50 (Expt#2), 100 (Expt#3), 200 (Expt#4) and 300 FPM (Expt# 5) were compared with baseline mats produced by UT (control), Neenah (Expt#1) and continuous carbon fiber composites. The detailed flexural and tensile properties are shown in figure 3 and 4. The panels from mats produced at 300 FPM (Expt#5) showed better flexural and tensile properties in comparison to mats produced at lower machine speeds.   From the data, the panels from mats produced at 300 FPM (Expt#5) showed better flexural and tensile properties in comparison to mats produced at lower machine speeds.

Basis weight: the panels from mats from 68 gsm (Expt#12) and 88 gsm (Expt#2) showed better flexural and tensile properties in comparison to mats produced at higher basis weight 178 gsm (Expt#7-1). It can be summarized that higher basis weight translates into lower mechanical properties.

Fiber length: the panels from mats produced using 12 mm fiber length (Expt#3) showed better flexural and tensile modulus in comparison to mats produced from 25 mm fiber length (Expt#11). Fiber entanglement due to increased fiber length in the mats results in lower modulus.

Repeatability: Data from two distinct sets of data conducted on different samples in widely separated calendar time showed that the mat intermediate fabrication processes were repeatable in a statistically significant sense.

Effect of sizing: no significant effect was observed on mechanical properties of the panels with and without sizing. This could be due to incompatibility of the sizing chemistries with the carbon fiber mats. Further investigation in choosing appropriate sizing chemistries is required.

10 RECOMMENDATIONS

To adopt to wet-laid process for forming carbon fibers mats, further modification of current pilot scale equipment is required that is originally designed for cellulosic fibers. Improvements are needed in bonding agent delivery system, pressing rollers, and drying system to handle the synthetic carbon fibers properly. Research is required to optimize equipment features in conjunction with process parameters.

11 REFERENCES

1) Senthil K, Punitha V. An Overview of Nonwoven Product Development and Modelling of Their Properties. J Text Sci Eng 2017;07. doi:10.4172/2165-8064.1000310.
2) Lin M-C, Lou C-W, Lin J-Y, Lin TA, Lin J-H. Tensile strength, peel load, and static puncture resistance of laminated composites reinforced with nonwoven fabric. J Mater Sci 2018;53:12145–56. doi:10.1007/s10853-018-2481-3.
3) Thomason JL. The influence of fibre length and concentration on the properties of glass fibre reinforced polypropylene: 5. Injection moulded long and short fibre PP. Compos Part A Appl Sci Manuf 2002;33:1641–52. doi:10.1016/S1359-835X(02)00179-3.
4) Andrić JS, Lindstrom SB, Sasic SM, Nilsson H. Particle-level simulations of flocculation in a fiber suspension flowing through a diffuser. Therm Sci 2017;21:S573–83. doi:10.2298/TSCI160510185A.
5) Yeole P, Ning H, Hassen AA, Vaidya UK. The Effect of Flocculent , Dispersants , and Binder on Wet – laid Process for Recycled Glass Fiber / PA6 Composite 2018;26:259–70.
6) Safavi A, Fathi S, Babaei MR, Mansoori Z, Latifi M. Experimental and numerical analysis of fiber characteristics effects on fiber dispersion for wet-laid nonwoven. Fibers Polym 2009;10:231–6. doi:10.1007/s12221-009-0231-5.
7) Yousfani SHS, Gong RH, Porat I. Manufacturing of fibreglass nonwoven webs using a paper making method and study of fibre orientation in these webs. Fibres Text East Eur 2012;91:61–7.

8) Guan X, Qian X, Yang Z. Comparison of several image analysis methods for fiber dispersion uniformity in water. J Dispers Sci Technol 2017;38. doi:10.1080/01932691.2015.1088455.

9) Fathi-Khalfbadam S, Latifi M, Sheikhzadeh-Najar S, Towhidkhah F. Analysis, and simulation of fiber dispersion in water using a theoretical analogous model. J Dispers Sci Technol 2011;32:352–8. doi:10.1080/01932691003659833.

10) Simmonds GE, Bomberger JD, Bryner MA. Designing Nonwovens to Meet Pore Size Specifications. J Eng Fiber Fabr 2007;2:1–15.

11) Wölling J, Schmieg M, Manis F, Drechsler K. Nonwovens from Recycled Carbon Fibres - Comparison of Processing Technologies. Procedia CIRP 2017;66:271–6. doi:10.1016/j.procir.2017.03.281.

12) Zhu G, Kremenakova D, Wang Y, Militky J. Air permeability of polyester nonwoven fabrics. Autex Res J 2015;15:8–12. doi:10.2478/aut-2014-0019.

13) Pierce RS, Falzon BG, Thompson MC. Permeability characterization of sheared carbon fiber textile preform. Polym Compos 2018;39:2287–98. doi:10.1002/pc.24206.

14) Stig F, Tahir MW, Åkermo M, Hallström S. An experimental study of the influence from fibre architecture on the permeability of 3D-woven textiles. J Reinf Plast Compos 2015;34:1444–53. doi:10.1177/0731684415593351.

15) Sharma S, Siginer DA. Permeability Measurement Methods in Porous Media of Fiber Reinforced Composites. Appl Mech Rev 2010;63:020802. doi:10.1115/1.4001047.

16) Endruweit A, Harper LT, Turner TA, Warrior NA, Long AC. the Permeability of Random Discontinuous Carbon Fibre Preforms n.d.:2–3.

17) Ghossein H, Hassen AA, Paquit V, Love LJ, Vaidya UK. Innovative Method for Enhancing Carbon Fibers Dispersion in Wet-Laid Nonwovens. Mater Today Commun 2018;17:100–8. doi:10.1016/j.mtcomm.2018.08.001.

12 APPENDIX A

Evaluation of Fiber Orientation

This appendix provides additional details pertaining to fiber orientation.

Figure 21 to 23 provide the process details, thermogravimetric analysis, and sizing process respectively.
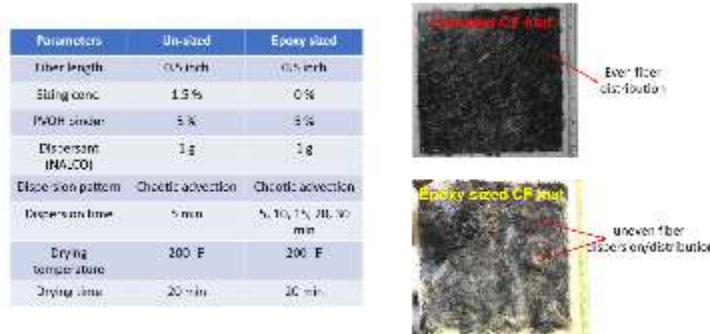
Figure 20.Process details for the fabrication of carbon fiber sized mats by UT team
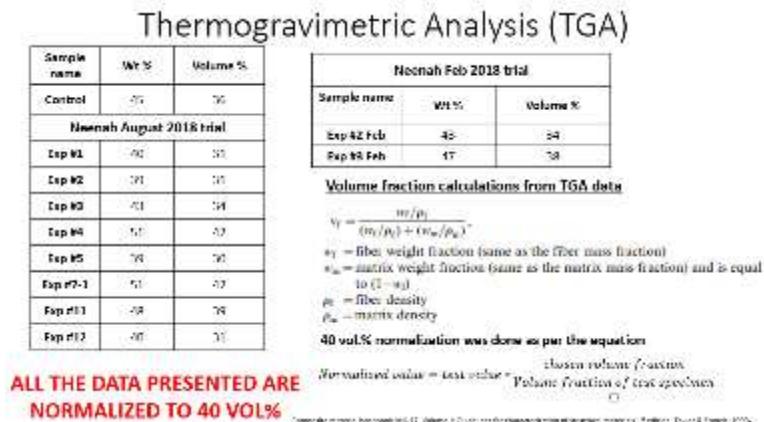
Figure 21.Thermogravimetric analysis and normalization data

Figure 22.Sizing process description

Experimental procedure for evaluating fiber orientation

- SURAGUS EddyCus CF map 5050iso system was used to determine the orientation and changes in the fiber alignment of the provided carbon fibers samples.
- All samples were measured in the machine direction. The results show that the first four samples are mainly isotropic while sample 5 has strong anisotropic properties.
- The samples show more horizontal and unidirectional distribution of angles and vectors maps.
- Sample 3 was measured in both MD and TD because the results are not matching the results of sample 1&2. The results indicate that the main fiber orientation is either transverse to sample 1&2 or that the sample was rotated prior labeling.
- The darker areas display less fibers and brighter areas display more fibers. Because no calibration of the FAW was applied the images show a relative FAW which is directly correlating with the sheet resistance of the plates. The different FAW values can be either caused by real FAW differences between the samples but also by different levels of compression and the different size of the samples. The relative FAW values of sample 1 to 3 can be directly compared.
- The results will be discussed with the customer in detail.

Samples : Five nonwoven mat samples were provided to SURAGUS. Two samples are cured and the other three are uncured. Machine direction of the five samples is marked on each sample. Figure 24 to 28 provide details of the equipment, fiber orientation and angle measurements in detail.

Measurement setup : EddyCus CF map 5050iso ; The samples have been measured with the SURAGUS Eddy current mapping system EddyCus CF map 5050iso. The EddyCus CF map 5050iso operates in the transmission mode. Four integrated sensors optimize the measuring process and provide non-contact measurement results. The scanning pitch was set to 1 mm in x- and 1 mm in y-direction. See Figure 25.

Figure 23.EddyCus CF map 5050iso.

Measurement results: To determine the information of the main fiber orientation, the samples have been measured in four sensor orientations (0, 45, 90 and 135°), the four different scans were combined with an algorithm afterwards. For best visibility, the information is shown in four different images:

1. Distribution of the main angle (Figure 25)
2. Anisotropy strength (Figure 26)
3. Sheet resistance and (Figure 27)
4. Vectors of the main angle for each location on the sample. (Figure 28)
5. Vector map of fiber orientation (Figure 29)

Their meanings are explained as following:
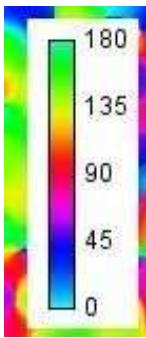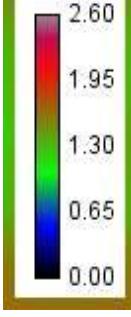
1) Distribution of the main angles	1) Anisotropy strength of the sample
The distribution of the main angles shows the fiber orientation in colors. Warm colors indicate vertical fiber orientation, cold colors horizontal fiber orientation. Blue = horizontal fiber orientation Red = vertical fiber orientation	The anisotropy strength of the sample is shown as a heat map. Warmer colors mean stronger anisotropy. Note that high anisotropy at the edges of the sample is a result of the measurement process (*edge effect*) and mathematic algorithm. Blue = isotropic (similar alignment in all direction) Red = anisotropic (strong orientation in one direction)
3) Fiber Areal Weight	4) Vectors of the main angles
This resulting image shows the average fiber areal weight. It shows less fibers with darker shades of gray (black) and more fibers with brighter shades of gray (white) White = high FAW Black = low FAW	The vector image shows a correlation between a location on the sample and the most present fiber orientation. The orientation and length of the vectors show the preferred direction of the fibers. Length (Vector) = Anisotropy strength Angle (Vector) = calculated dominant orientation

Figure 24.Angles Map and Histogram of Angles Map

Sample 1_MD	
	Count: 1210000 Min: 4.062E-15 Mean: 107.190 Max: 179.979 StdDev: 85.271 Mode: 1.758 (90813) Bins: 256 Bin Width: 0.703
Sample 2_MD	
	Count: 1210000 Min: 4.130E-15 Mean: 98.853 Max: 179.972 StdDev: 86.143 Mode: 0.352 (91772) Bins: 256 Bin Width: 0.703
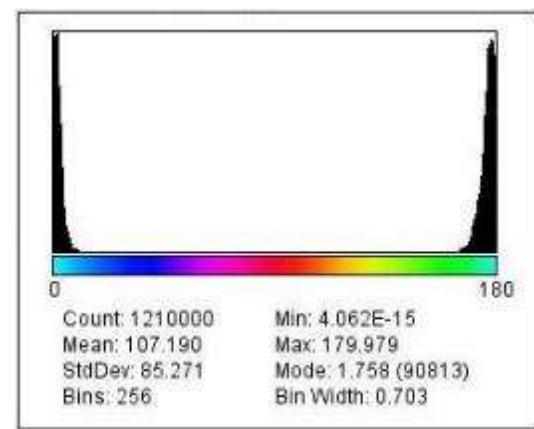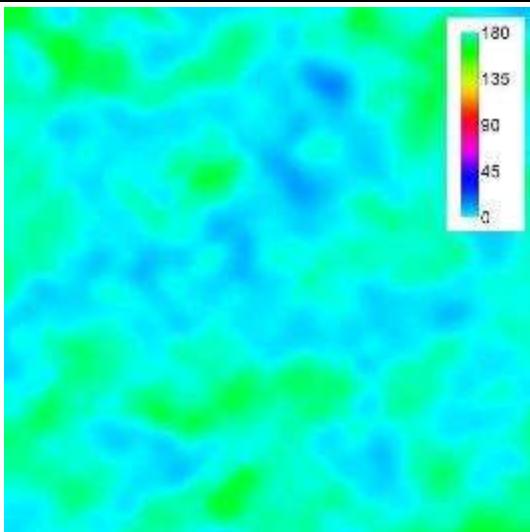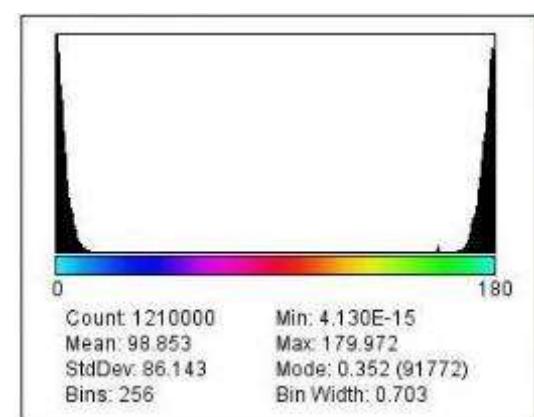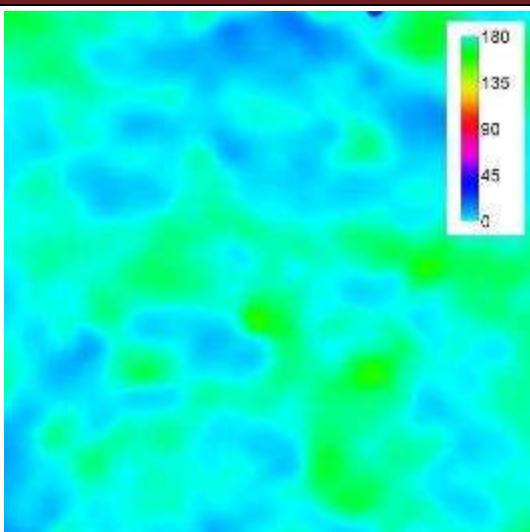
Figure 25.Anisotropy Strength and Histogram of Anisotropy Strength

Sample 3_MD	
	 Count: 1440000 Min: 65.445 Mean: 96.144 Max: 128.339 StdDev: 7.154 Mode: 94.570 (89078) Bins: 256 Bin Width: 0.703
Sample 3_TD	
	 Count: 1440000 Min: 3.343E-15 Mean: 55.121 Max: 179.964 StdDev: 78.219 Mode: 3.867 (96295) Bins: 256 Bin Width: 0.703

Figure26 (Continued) Anisotropy Strength and Histogram of Anisotropy Strength

Sample 4_MD	

Count: 1000000   Min: 3.508E-15
Mean: 100.670   Max: 179.540
StdDev: 82.683   Mode: 0.352 (70156)
Bins: 256   Bin Width: 0.703

Sample 5_MD	

Count: 1210000   Min: 4.078E-15
Mean: 103.001   Max: 179.509
StdDev: 86.743   Mode: 0.352 (272565)
Bins: 256   Bin Width: 0.703

Figure26 (Continued) Anisotropy Strength and Histogram of Anisotropy Strength

Sample 1_MD	
	Count: 1210000 Min: 0.133 Mean: 0.408 Max: 0.775 StdDev: 0.0872 Mode: 0.372 (36256) Bins: 256 Bin Width: 0.00586
Sample 2_MD	
	Count: 1210000 Min: 0.0184 Mean: 0.342 Max: 0.601 StdDev: 0.0771 Mode: 0.343 (41124) Bins: 256 Bin Width: 0.00586

Figure26 (Continued) Anisotropy Strength and Histogram of Anisotropy Strength

Sample 3_MD

Count: 1440000	Min: 0.0726	
Mean: 0.235	Max: 0.426	
StdDev: 0.0719	Mode: 0.282 (41445)	
Bins: 256	Bin Width: 0.00547	

Sample 3_TD

Count: 1440000	Min: 0.0963	
Mean: 0.278	Max: 0.480	
StdDev: 0.0672	Mode: 0.296 (45019)	
Bins: 256	Bin Width: 0.00586	

Figure26 (Continued) Anisotropy Strength and Histogram of Anisotropy Strength

Sample 4_MD	

Count: 1000000   Min: 0.0319
Mean: 0.160   Max: 0.347
StdDev: 0.0490   Mode: 0.179 (58864)
Bins: 256   Bin Width: 0.00586

Sample 5_MD	

Count: 1210000   Min: 0.300
Mean: 0.949   Max: 1.400
StdDev: 0.128   Mode: 0.999 (86501)
Bins: 256   Bin Width: 0.00586

Figure26 (Continued) Anisotropy Strength and Histogram of Anisotropy Strength

|	anisotropy	histogram of orientation
Sample 1 MD		
Sample 2 MD		
Sample 3 MD		
Sample 4 MD		
Sample 5 MD		

Figure 26.Fiber Areal Weight and Histogram of FAW
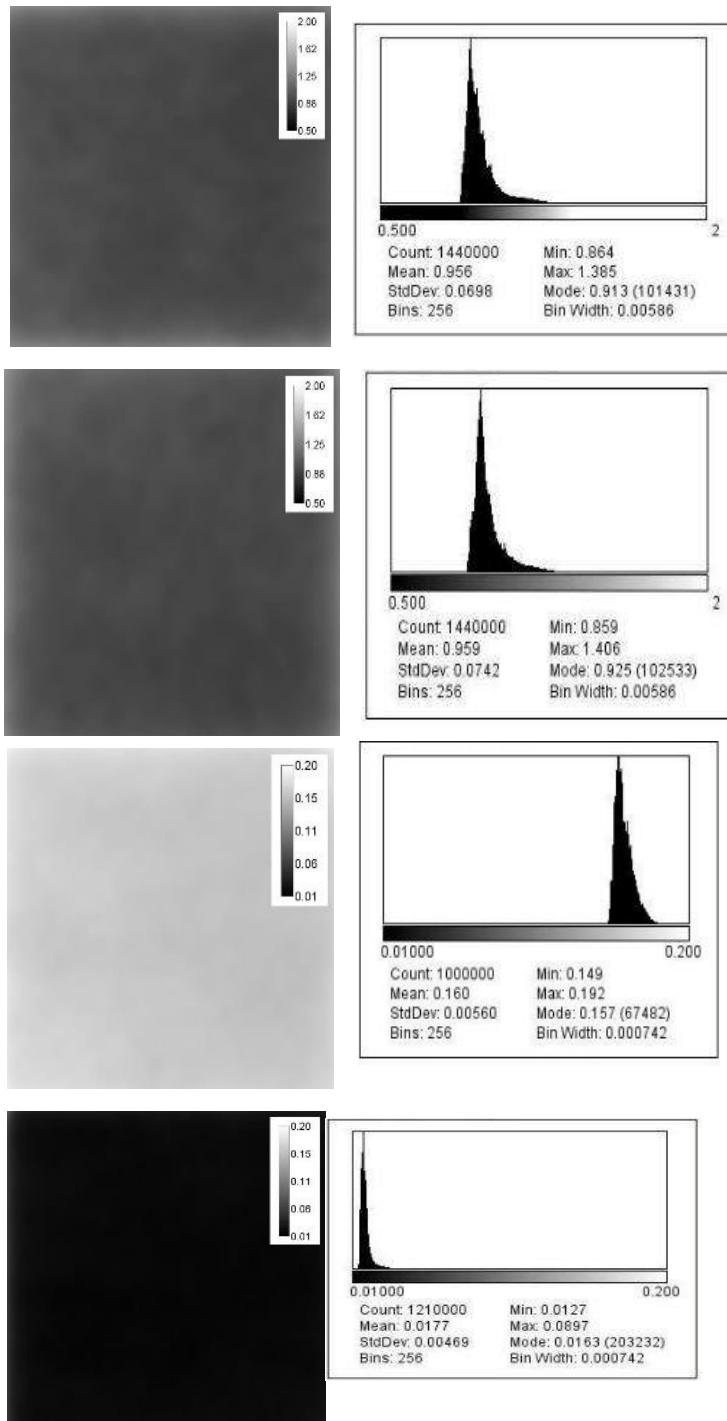
Figure 27.Mean values of Anisotropy, Vector maps and FAW

Table 6 Vector Data

Sample ID	Sample 1 MD	Sample 2 MD	Sample 3 MD	Sample 3 TD	Sample 4 MD	Sample 5 MD
Mean Anisotropy Strength Values	0.41	0.34	0.24	0.28	0.16	0.95

Sample ID	Sample 1 MD	Sample 2 MD	Sample 3 MD	Sample 3 TD	Sample 4 MD	Sample 5 MD
Mean vectors distribution	7.79	6.51	4.45	5.30	3.03	13.54

Sample ID	Sample 1 MD	Sample 2 MD	Sample 3 MD	Sample 3 TD	Sample 4 MD	Sample 5 MD
Mean FAW Values	1.18	1.03	0.96	0.96	0.16	0.18

| Sample 1_MD	Sample 2_MD
Sample 3_MD	Sample 3_TD
Sample 4_MD	Sample 5_MD
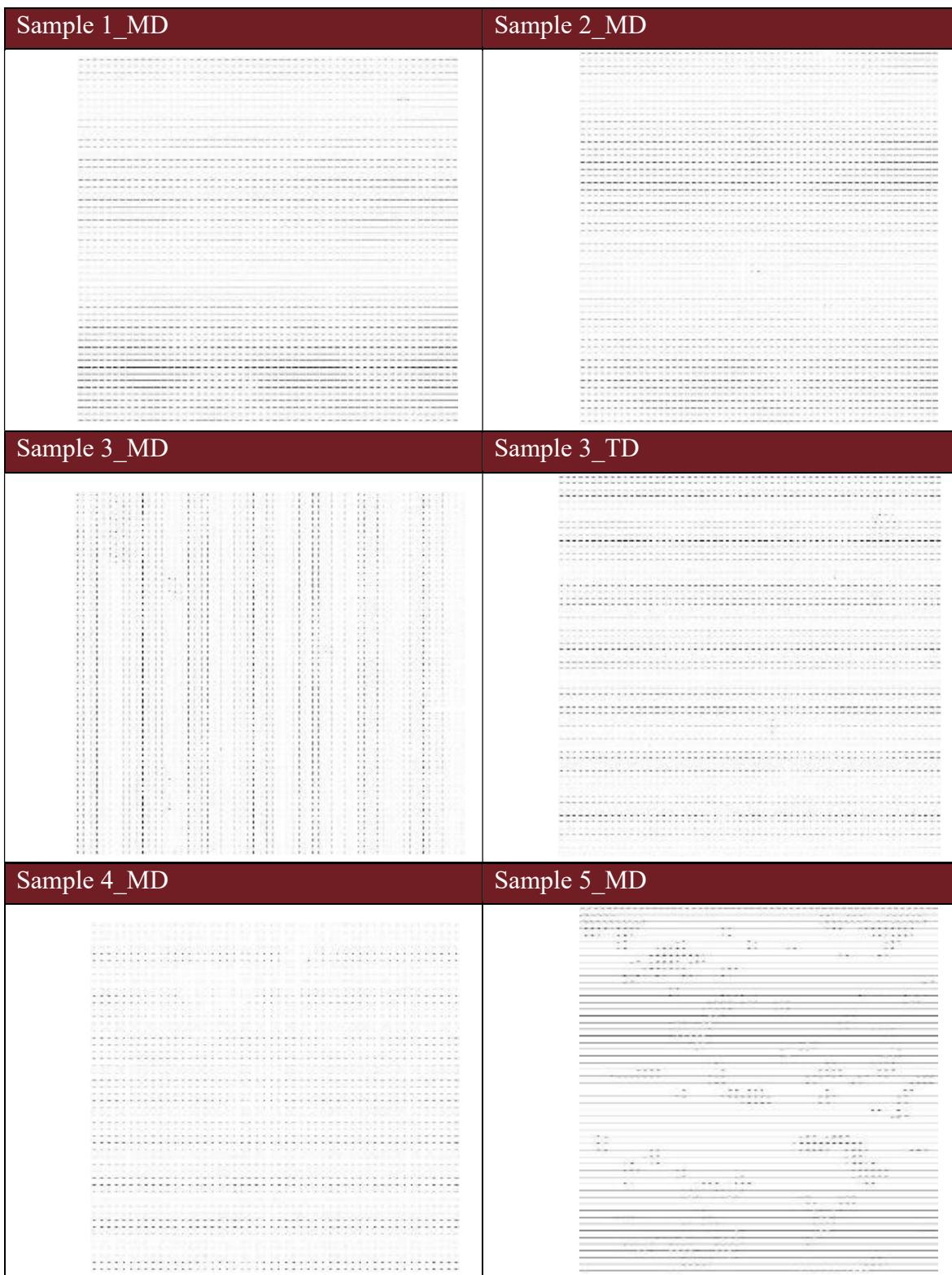
Figure 28.Vector map of fiber orientation